Kinetics and Thermodynamics of Intermolecular Catalysis by Hairpin Ribozymes†

Lisa A. Hegg and Martha J. Fedor*

Department of Biochemistry and Molecular Biology, University of Massachusetts Medical Center, 55 Lake Avenue North, Worcester, Massachusetts 01655-0103

Received July 10, 1995; Revised Manuscript Received September 20, 1995⊗

ABSTRACT: The hairpin ribozyme, derived from the negative strand of the satellite RNA of tobacco ringspot virus, belongs to the class of small catalytic RNAs that cleave RNA to generate 2′,3′-cyclic phosphate and 5′-hydroxyl termini and ligate these termini in the reverse reaction to form 3′,5′-phosphodiesters. Rate and equilibrium constants for binding, dissociation, cleavage, and ligation steps in the kinetic mechanism were determined using a series of hairpin ribozyme/substrate pairs that differed in the sequence and length of the intermolecular base-paired helices. All hairpin variants cleaved with rate constants of ~0.3 min^{-1} at pH 7.5 in 10 mM $MgCl_2$ at 25 °C, regardless of the length or sequence of the intermolecular helices. A rate constant of ~3 min^{-1} was determined for an intermolecular ligation reaction in which both cleavage products were supplied to the ribozyme in *trans*. Thus, the hairpin favored ligation over cleavage by 10-fold when the ribozyme was saturated with cleavage products. Binding rate constants for cleavage substrates and products were comparable to values reported for other catalytic RNAs but were somewhat slower than binding rates typical of small RNA helices. Substrate dissociation rate constants were much slower than cleavage rate constants for all substrates. Because virtually every substrate that was bound was cleaved before it could dissociate, K_M^S values were not the same as K_d^S values. Instead, K_M^S reflected the ratio of cleavage and substrate binding rate constants and had the same value of ~30 nM for all substrates. Calculations based on empirically determined free energy parameters for simple RNA helices indicated that complexes between ribozymes and 5′-cleavage products were slightly less stable than simple helices with the same sequences. In contrast, affinities between ribozymes and cleavage substrates and between ribozymes and 3′-cleavage products were stronger than expected for simple duplexes by about −2.5 kcal/mol, evidence of stabilizing interactions in addition to those contributed by helical base pairs. This kinetic and thermodynamic study demonstrates that the kinetic mechanism of the hairpin ribozyme is distinct from the kinetic mechanisms of other well-characterized ribozymes and provides a foundation for further exploration of the hairpin structure and catalytic mechanism.

Multimeric intermediates in rolling circle replication of several plant virus satellite RNAs are processed into smaller linear and circular genomes through RNA-catalyzed self-cleavage and ligation reactions (Prody et al., 1986; Buzayan et al., 1986a,b; Hutchins et al., 1986). The negative strand of the satellite RNA of tobacco ringspot virus [(−)sTRSV][1] contains a small (<80 nt) catalytic domain termed the "hairpin" (Buzayan et al., 1986a,b; Hampel & Tritz, 1989; Haseloff & Gerlach, 1989; Feldstein et al., 1989). Along with the hammerhead and axehead catalytic RNAs, the hairpin belongs to the family of small RNA endonucleases which reversibly cleave phosphodiesters to generate 5′-hydroxyl and 2′,3′-cyclic phosphate termini [for review, see Symons, (1992) and Long and Uhlenbeck (1993)]. Although these domains assemble from sequences within a single RNA *in vivo*, each domain can also assemble from separate ribozyme and substrate RNAs which associate, at least in part, through complementary base pairs (Sampson et al., 1987; Uhlenbeck, 1987; Haseloff & Gerlach, 1988; Koizumi et al., 1988a,b; Jeffries & Symons, 1989; Hampel & Tritz, 1989; Perrota & Been, 1992). Intermolecular configurations facilitate application of conventional enzymological methods to studies of kinetic and chemical mechanisms and the design of antisense ribozymes for gene inactivation applications.

A hairpin secondary structure model composed of two pairs of helix−loop−helix segments (Figure 1A; Hampel & Tritz, 1989) has been supported by truncation (Feldstein et al., 1989), mutagenesis (Haseloff & Gerlach, 1989; Hampel et al., 1990; Chowrira & Burke, 1991; Anderson et al., 1994), primer extension (Feldstein et al., 1990), phylogenetic comparison (Haseloff & Gerlach, 1988; Rubino et al., 1990), *in vitro* selection (Berzal-Herranz et al., 1992, 1993; Joseph et al., 1993), cross-linking (Vitorino Dos Santos et al., 1993; Butcher & Burke, 1994a), and chemical protection (Butcher & Burke, 1994b) studies. A symmetrical internal loop in the base of the hairpin stem contains the reactive phosphodiester. Most helical portions of the domain tolerate base pair substitutions without loss of activity, while alteration of most loop nucleotides interferes with catalysis. The asymmetrical internal loop shows homology to a conserved motif found in ribosomal and viroid RNAs (Butcher & Burke, 1994a). Cross-linking (Vitorino Dos Santos et al., 1993; Butcher & Burke, 1994a), chemical protection studies (Butcher & Burke, 1994a,b), and functional assays with modified oligonucleotides (Grasby et al., 1995) provide evidence for non-Watson−Crick base pairing among loop nucleotides. While

† This work was supported by NIH Grant GM 46422 to M.J.F. L.A.H. was the recipient of NIH Fellowship GM 15912.

* Author to whom correspondence should be addressed.

⊗ Abstract published in *Advance ACS Abstracts,* November 1, 1995.

[1] Abbreviations: (−)sTRSV, negative strand of the satellite RNA of tobacco ringspot virus; Tris, tris(hydroxymethyl)aminomethane; EDTA, (ethylenedinitrilo)tetraacetic acid; TBE, 50 mM Tris-borate, pH 8.3, 1 mM EDTA; MES, 2-(*N*-morpholino)ethanesulfonic acid.

0006-2960/95/0434-15813$09.00/0

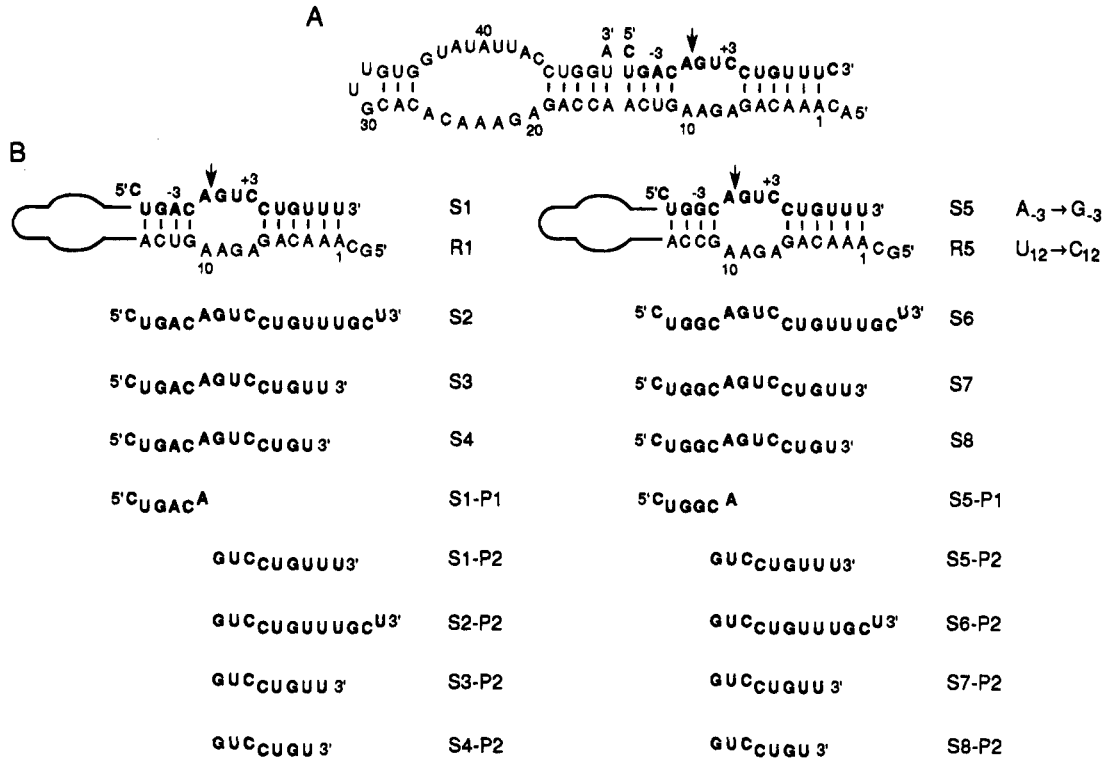

FIGURE 1: Hairpin sequences. A, sequence and secondary structure model of the (−)sTRSV hairpin ribozyme−substrate complex (Hampel & Tritz, 1989; Feldstein et al., 1989; Haseloff & Gerlach, 1989; Hampel et al., 1990; Rubino et al., 1990; Chowrira & Burke, 1991; Berzal-Herranz et al., 1993; Joseph et al., 1993; Butcher & Burke, 1994a,b). Sequences are numbered according to Chowrira and Burke (1991). Substrate nucleotides are in bold font, and the reactive phosphodiester is indicated by an arrow. B, sequences of hairpin ribozyme (R), substrate (S), 5′-cleavage product (P1), and 3′-cleavage product (P2) RNAs used in this study. S1−P1 and S5−P1 are the 5′-products of R1- or R5-mediated cleavage, respectively, and have 2′,3′-cyclic phosphate termini. The 3′-products of R1-mediated cleavage, S1−P2, S2−P2, S3−P2, and S4−P2, are identical to S5−P2, S6−P2, S7−P2, and S8−P2, respectively, but the latter RNAs are products of R5−mediated cleavage. Except for the indicated changes in the sequence of the P1 helices and the length of the P2 helices, all RNAs have the same sequence as the hairpin domain of (−)sTRSV.

no specific interactions between the two helix−loop−helix domains have been identified, the two domains are thought to adopt a noncoaxial "paper clip" structure and associate through additional tertiary interactions (Feldstein & Bruening, 1993; Komatsu et al., 1994).

Hairpin and hammerhead ribozymes catalyze the same reactions and are derived from opposite strands of the same satellite RNA yet appear to use distinct mechanisms. Early observations that the ratio of linear to circular satellite RNAs *in vivo* was higher for the (+) strand than for the (−) strand of sTRSV suggested that cleavage was favored over ligation by the hammerhead but not the hairpin domain (Buzayan et al., 1986b, 1988; van Tol et al., 1991). The hammerhead has since been shown to catalyze ligation *in vitro* at less than one-hundredth of the rate of cleavage (Hertel et al., 1994; Hertel & Uhlenbeck, 1995). In contrast, the hairpin domain catalyzes ligation readily *in vitro* (Feldstein & Bruening, 1993; Komatsu et al., 1993), and the ability of the hairpin to acquire a selectable sequence through ligation has been exploited for identification of functional hairpin sequence variants (Berzal-Herranz et al., 1992, 1993; Joseph et al., 1993). While the hammerhead reaction is completely dependent on divalent ions (Dahm et al., 1993), hairpin catalysis has been reported in the absence of added divalent ions, although catalytic efficiency was significantly reduced (Forster et al., 1987; Chowrira et al., 1993). Finally, substitution of a *pro-Rp* phosphorothioate for the reactive phosphate had little effect on hairpin catalysis (Buzayan et al., 1988; Chowrira & Burke, 1991) while the same substitution changes the divalent ion specificity of the hammerhead reaction, evidence of direct coordination of a divalent ion to the reactive phosphate (Dahm & Uhlenbeck, 1991). The molecular basis for these apparent differences in kinetic and chemical mechanisms between hairpin and hammerhead ribozymes is not yet understood.

Kinetic and thermodynamic analyses of intermolecular reactions of hammerhead ribozymes (Fedor & Uhlenbeck, 1990, 1992; Hertel et al., 1994; Hertel & Uhlenbeck, 1995) and the mechanistically distinct Group I intron-derived (Herschlag & Cech, 1990; Pyle et al., 1990; Zaug et al., 1994), Group II intron-derived (Franzen et al., 1993; Pyle & Green, 1994), and RNase P (Smith & Pace, 1993; Beebe & Fierke, 1994) ribozymes have facilitated studies of mechanistic and structural features of these catalytic domains [reviewed in Symons (1992), Long and Uhlenbeck (1993), Cech, (1993), and Pyle (1993)]. Reaction rates for hairpin domains have been reported by several groups (Feldstein et al., 1989; Hampel & Tritz, 1989; Hampel et al., 1990; Chowrira & Burke, 1991; Chowrira et al., 1993; Feldstein & Bruening, 1993). The present study extends these observations using a combination of steady-state and pre-steady-state kinetic and equilibrium assays to define rate and equilibrium constants for individual steps in the kinetic mechanism. Hairpin reactions were assayed in 50 mM Tris, pH 7.5, 10 mM $MgCl_2$, at 25 °C to allow direct comparison with hammerhead-catalyzed reactions (Fedor & Uhlenbeck, 1990, 1992; Hertel et al., 1994; Hertel & Uhlenbeck, 1995). Rate and equilibrium constants for intermolecular catalysis

by the hairpin ribozyme are reported here to provide a foundation for detailed mechanistic and structural studies and to facilitate design of antisense hairpin ribozymes.

EXPERIMENTAL PROCEDURES

Preparation of RNAs. Ribozyme RNAs (Figure 1B) were synthesized by T7 RNA polymerase transcription of partially duplex synthetic DNA templates (Milligan et al., 1987) and purified by denaturing gel electrophoresis as previously described (Fedor & Uhlenbeck, 1990). Substrate and product RNAs were synthesized chemically, deprotected, desalted, and gel purified as previously described (Fedor & Uhlenbeck, 1992). Concentrations were determined by assuming a residue extinction coefficient of 6.6×10^3 M^{-1} cm^{-1} at 260 nm. The correct 3′-terminal nucleotide was confirmed for transcripts by complete nuclease digestion of [5′-^{32}P]pCp 3′-end-labeled material (England & Uhlenbeck, 1988) and two-dimensional thin-layer chromatography (Kochino et al., 1980). Ribozyme (R), substrate (S), 5′-product (P1), and 3′-product (P2) RNAs were also subjected to partial alkaline hydrolysis and sequenced by partial enzymatic hydrolysis to confirm length and sequence. After some experiments, ribozymes were recovered from analytical gels, purified, and used for further experiments with no detectable effect on kinetics or equilibrium measurements.

Preparation of 5′-cleavage products with the appropriate 2′,3′-cyclic phosphate termini began with the chemical synthesis of S1−P1 and S5−P1 RNA sequences but with an extra guanosine at the 3′-end. Periodate oxidation and β-elimination of the 3′-terminal guanosine produced 3′-phosphate termini which were then condensed with 1-ethyl-3-[3-(dimethylamino)propyl]carbodiimide to yield the 2′,3′-cyclic phosphate (Naylor & Gilham, 1966; Hertel et al., 1994). Product RNAs that were generated through ribozyme-mediated cleavage were indistinguishable from RNAs prepared through chemical modification in kinetics and equilibrium binding experiments.

[5′-^{32}P]RNAs were prepared by reaction with T4 polynucleotide kinase and [γ-^{32}P]ATP as previously described (Fedor & Uhlenbeck, 1990). For experiments that required ^{32}P-labeled 3′-cleavage products with 5′-OH termini, [5′-^{32}P]-pUp was ligated to RNA that was identical in sequence to P2 but that lacked the 3′-terminal uridine (England & Uhlenbeck, 1988). [5′-^{32}P]pUp was synthesized by incubating 6 μM Up, 300−600 μCi of [γ-^{32}P]ATP, and 1 unit of T4 polynucleotide kinase/μL in 50 mM Tris, pH 7.6, 10 mM $MgCl_2$, 5 mM spermidine, 0.1 mM EDTA, 5 mM DTT at 37 °C for 1.5 h. [3′-^{32}P]P2 was prepared by incubating 15 μL of [5′-^{32}P]pUp, 0.2 μM P2 lacking the 3′-terminal uridine, 100 μM ATP, 10% DMSO, and 2.5 units of T4 RNA ligase/mL in 50 mM HEPES-OH, pH 8.3, 10 mM $MgCl_2$, 3 mM DTT, in a total volume of 60 μL at 15 °C for 12−16 h. [^{32}P]RNAs were purified from labeling reactions by denaturing gel electrophoresis as described above, and concentrations were calculated from the specific activity of the [γ-^{32}P]ATP used for labeling which was 3000−5000 Ci/mmol.

Kinetics. Unless otherwise indicated, reactions were carried out in 50 mM Tris-HCl, pH 7.5, 10 mM $MgCl_2$ at 25 °C, conditions identical to those used previously to determine hammerhead rate and equilibrium constants (Fedor & Uhlenbeck, 1990, 1992; Hertel et al., 1994). Separate solutions of ribozyme, substrate, and product RNAs were heated to 100 °C to disrupt any aggregates that might have formed during storage (Groebe & Uhlenbeck, 1988). RNAs were cooled to 25 °C, adjusted to a final concentration of 10 mM $MgCl_2$, and equilibrated at 25 °C for 10 min or longer. Reactions were initiated by mixing ribozyme with substrate or product RNAs. Samples were removed at intervals, quenched with an equal volume or more of 7 M urea, 50 mM EDTA, 0.002% bromophenol blue, and 0.002% xylene cyanole and fractionated on 20% acrylamide, 7 M urea gels. Radioactivity in product and substrate bands was quantitated by scintillation counting of excised bands or by radioanalytic scanning with a Molecular Dynamics PhosphorImager. Values obtained from similar experiments typically varied less than 2-fold.

Cleavage Reactions. Kinetic parameters for substrate cleavage were determined from single-turnover reactions as previously described (Fedor & Uhlenbeck, 1992). Briefly, reactions contained ribozyme, at eight or more concentrations ranging from 0.1 to 1000 nM, and [5′-^{32}P]substrate, at concentrations that were at least 10-fold lower than the ribozyme concentrations. Observed cleavage rates were obtained from fits of ln(fraction S) versus time for each ribozyme concentration after normalization to the fraction of product measured at the end of the reaction which was typically 0.6 for R1 substrates and 0.8 for R5 substrates. Plots of $k_{obs,\ cleavage}$ versus $k_{obs,\ cleavage}$/[R] were used to calculate K_M^S values and cleavage rate constants, k_2 (Eadie, 1942; Hofstee, 1952). Because these reactions were carried out with ribozyme in excess rather than substrate in excess, K_M^S is not a true Michaelis constant but describes the ribozyme concentration at which the reaction velocity was half-maximal.

In substrate-excess cleavage reactions, ribozyme, at concentrations ranging from 1 to 20 nM, was combined with [5′-^{32}P]substrate at concentrations that were at least 20-fold higher. Single- and multiple-turnover cleavage rates were calculated from linear fits of [P]/[R] versus time during the initial phase of the reaction, when less than 15% of the substrate had been converted to product. Plots of k_{obs} versus k_{obs}/[S] were used to calculate K_M^S and k_{cat} values.

Ligation Reactions. Kinetic parameters for product ligation were determined from single-turnover reactions in which a small amount of radioactive 5′-cleavage product, [5′-^{32}P]-P1, was combined with various concentrations of a complex that contained both ribozyme and the 3′-cleavage product, S2−P2. A solution of ribozyme, at concentrations ranging from 0.05 to 30 μM, and a 10% excess of S2−P2 was heated to 100 °C, cooled to 25 °C, and adjusted to a final concentration of 10 mM $MgCl_2$. Complex formation between the ribozyme and S2−P2 was expected to be complete at these concentrations. The R·P2 complex was then added to a trace amount of [5′-^{32}P]P1 to initiate the reaction. Samples were quenched at intervals, and the fraction of ligated [5′-^{32}P] substrate was measured. Observed ligation rates were determined from exponential fits of fraction S versus time. K_M^{P1} and ligation rate constants, k_{-2}, were obtained from the fit to $k_{obs,\ ligation} = k_{-2}([E{\cdot}P2]/([E{\cdot}P2] + K_M^{P1})) + k_2$, where $[E{\cdot}P2] = [E]_{total}$, as described under Results. Doubling the concentration of [5′-^{32}P]P1 had no effect on ligation rates, confirming that [5′-^{32}P]P1 concentrations were low relative to the concentration of the R·P2 complex. P1 RNAs with 2′,3′-cyclic phosphate termini

generated through β-elimination and condensation were kinetically indistinguishable from P1 RNAs generated through ribozyme-mediated substrate cleavage.

Equilibrium Binding Assays. Equilibrium dissociation constants for complexes between ribozymes and cleavage products were measured using nondenaturing gel shift assays similar to those previously used to measure equilibrium dissociation constants for RNA complexes (Pyle et al., 1990; Fedor & Uhlenbeck, 1992). Briefly, a small amount of [^{82}P]product was combined with ribozyme at a range of concentrations that were at least 10-fold higher. Solutions were adjusted to a final concentration of 10 mM $MgCl_2$, 5% sucrose (w/v), 0.002% bromophenol blue, and 0.002% xylene cyanol and were equilibrated at 25 °C for times ranging from 18 h to 3 days. Reactions that were equilibrated for longer and shorter times were compared to ensure that equilibrium was achieved. Bound and unbound ligands were fractionated using 15% acrylamide gels in 50 mM Tris acetate, pH 7.5, 10 mM magnesium acetate buffer. The fraction of bound ligand (FB) was plotted as a function of ribozyme concentration, and K_d values were calculated by fitting to $FB_\infty = [R]/([R] + K_d)$.

Product Binding and Dissociation Reactions. Rate constants for binding, k_{-4}, and dissociation, k_4, of 3′-cleavage products, P2, were measured using pulse−chase electrophoresis experiments like those described by Hertel et al. (1994). To measure product dissociation rate constants, a small amount of [3′-^{32}P]P2 or [5′-^{32}P]P2 was first combined with a saturating concentration of ribozyme. After 10 min, a sample of the binding reaction was loaded onto a running nondenaturing gel to measure the fraction of [^{32}P]P2 bound at t_0, which was typically 0.9 or more. The remainder was diluted into a 200-fold excess of nonradioactive P2 to prevent rebinding of any [^{32}P]P2 that dissociated. At various intervals after dilution, free and bound [^{32}P]P2 were fractionated on nondenaturing gels. Rate constants for P2 dissociation, k_4, were determined by exponential fits to the fraction bound versus time after normalization to the amount of bound [^{32}P]P2 measured at t_0. When ribozyme was combined with nonradioactive P2 before [^{32}P]P2 was added, in control experiments, less than 2% of [^{32}P]P2 was bound after 2.5 h, evidence that the concentration of nonradioactive P2 present during the chase was sufficient to prevent rebinding of [^{32}P]-P2.

To measure rate constants for product binding, k_{-4}, [5′-^{32}P]P2 or [3′-^{32}P]P2, at concentrations less than 0.01 nM, was combined with ribozyme at concentrations ranging from 0.1 to 1 nM. After various times, binding reactions were quenched by 10-fold dilution into a solution of 600 nM S2−P2, 50 mM Tris-HCl, pH 7.5, 10 mM $MgCl_2$, 5% sucrose (w/v), 0.002% bromophenol blue, and 0.002% xylene cyanole and loaded onto 15% acrylamide gels in 50 mM Tris-acetate, pH 7.5, 10 mM magnesium acetate buffer. The observed rate of binding at each ribozyme concentration was determined from the fraction of ribozyme-bound [^{32}P]P2 after various times. Binding and dissociation rate constants were described by the slope and *Y*-intercept, respectively, of plots of $k_{obs,\ binding}$ versus [R] based on the relationship $k_{obs,\ binding} = k_{-4}[R] + k_4$.

Substrate Dissociation Reactions. Substrate dissociation rate constants were assayed by comparison to cleavage rate constants using two types of experiments. In partitioning experiments (Rose et al., 1974) similar to those used to assay substrate dissociation for the *Tetrahymena* Group I-derived and hammerhead ribozymes (Herschlag & Cech, 1990; Fedor & Uhlenbeck, 1992; Hertel et al., 1994), [5′-^{32}P]substrate and ribozyme were combined during an initial binding period, diluted to prevent further binding, and then monitored through a chase period to compare the fraction of substrate that remained bound and cleaved to the fraction that escaped cleavage by dissociating. A small amount of [5′-^{32}P]substrate was first combined with ribozyme, at a concentration of 1 μM or higher, and was incubated for an initial binding period, t_1, of 1−4 min. All substrate was expected to form complex by the end of t_1 at these ribozyme concentrations and binding times. Solutions were then diluted 5000-fold into 50 mM Tris-HCl, pH 7.5, 10 mM $MgCl_2$, to prevent rebinding of any dissociated substrate, and the amount of [5′-^{32}P]product was measured after various chase intervals, t_2. Substrate dissociation rate constants, k_{-1}, were calculated by comparing the rate and extent of cleavage in the chased reaction to a control reaction without the chase, as described previously (Fedor & Uhlenbeck, 1992) and in Results. In a variation of this experiment, a 95 °C incubation and preannealing step was incorporated into the binding reaction, as described under Results.

In the second type of partitioning experiment, the [^{32}P]-substrate-ribozyme complex was formed through ribozyme-mediated ligation of product RNAs rather than through a substrate-binding reaction. Briefly, 1 μL of [5′-^{32}P]P1 was combined with 2.0 μL of 15 μM R·S2−P2 in 50 mM Tris-HCl, 10 mM $MgCl_2$, for an initial ligation period, t_1, of 1−10 min. The amount of radioactive P1 converted to substrate during t_1 ranged from 15% to 30%. Ligation reactions were then diluted into 10 mL 50 mM Tris-HCl, pH 7.5, 10 mM $MgCl_2$, to prevent further ligation or binding and cleavage of any dissociated substrate. The amount of radioactivity in substrates and products was measured after various chase intervals, t_2, which spanned at least six times the $t_{1/2}$ for the cleavage reaction. Substrate dissociation rate constants were calculated from the rate and extent of substrate cleavage during t_2 as described in Results. Less than 1% of [5′-^{32}P]-P1 was converted to substrate by the end of the chase in control experiments in which the R·P2 complex was diluted into the chase solution before [5′-^{32}P]P1 was added, confirming that chase conditions prevented further [5′-^{32}P]P1 binding and ligation. Likewise, when [5′-^{32}P]substrate was added to the chase solution before ribozyme, no cleavage was detected, indicating that any substrate that dissociated during the chase would be unable to rebind or cleave.

RESULTS

The hairpin domains examined in these studies (Figure 1B) are derived from the autocatalytic domain of (−)sTRSV but assemble from separate ribozyme and substrate RNAs. Ribozymes (R) cleave substrates (S) to yield a 5′-cleavage product (P1) and a 3′-cleavage product (P2) which are ligated to form substrate in the reverse reaction. Substrates and products associate with ribozymes through the P1 and P2 base-paired helices which flank a symmetrical loop containing the reactive phosphodiester. The R1/S1 hairpin has the same sequence as the autocatalytic domain of (−)sTRSV except that the 5′-terminal nucleotide of R1 is a guanosine rather than an adenosine. Reactions of hairpin sequences very similar to R1/S1 have been characterized previously (Feldstein et al., 1989; Hampel & Tritz, 1989; Hampel et

al., 1990; Chowrira & Burke, 1991; Sekiguchi et al., 1991; Chowrira et al., 1993; Feldstein & Bruening, 1993; Komatsu et al., 1993, 1994). A series of hairpin sequences was designed to vary the stability of the intermolecular P1 and P2 helices so that binding and dissociation rate and equilibrium constants for substrates and products would fall into a measurable range (Figure 1B). The R1/S2 hairpin is the same as R1/S1 except that the P2 helix of R1/S2 is extended by two G·C base pairs and S2 has an unpaired 3′-terminal uridine. S3 and S4 are shorter than S1 by one or two uridine residues, respectively, so that the P2 helices of R1/S3 and R1/S4 lack one or two U·A base pairs compared to R1/S1. An A_{-3}·U_{12} pair in the P1 helix of R1/S1 was changed to a G_{-3}·C_{12} pair to create R5/S5. R5/S6, R5/S7, and R5/S8 have the same P1 helix as R5/S5, but R5/S6 has the extended P2 helix of R1/S2 and the R5/S7 and R5/S8 hairpins have the shorter P2 helices of R1/S3 and R1/S4, respectively.

Several criteria were used to identify substrate and ribozyme sequences that were suitable for kinetic analysis and a number of sequence alterations that were tested yielded nonfunctional RNAs. Because self-association of oligoribonucleotides has been shown to complicate kinetic analysis of hammerhead ribozymes (Fedor & Uhlenbeck, 1990), nondenaturing gel electrophoresis was used to assess structural homogeneity. An *in vitro* transcript with the same sequence as S1, but with two unpaired 5′-terminal nucleotides, gave rise to multiple slowly migrating species on nondenaturing gels and was not used for further experiments. S2 and S6 RNAs produced multiple species at concentrations above 50 nM, so experiments with these substrates were performed below this concentration. Ribozyme RNAs migrated as single species at concentrations below 1 μM. A lower mobility species was detected at concentrations above 1 μM, which likely corresponds to a ribozyme aggregate previously identified in cross-linking experiments (Butcher & Burke, 1994a). The fraction of ribozyme in this lower mobility species was no more than 13% at the highest ribozyme concentrations used for kinetic and equilibrium binding experiments, as described below. The remaining RNAs migrated as single species on nondenaturing gels at the highest concentrations that could be tested without overloading gels. No conformational heterogeneity was detected by nondenaturing gel analysis of an RNA that was identical to S1 except that it lacked the unpaired 5′-terminal cytosine, but reactions with the shorter substrate displayed anomalous kinetics. At low concentrations, the shorter substrate cleaved at rates similar to rates observed with substrates that had an unpaired 5′-terminal cytosine, but cleavage rates failed to increase with increasing concentrations as expected. Furthermore, substrate lacking the 5′-terminal cytosine inhibited cleavage of an otherwise reactive substrate in a concentration-dependent fashion, indicating that the shorter substrate bound ribozyme at high concentrations but failed to cleave (data not shown). Due to the apparent propensity of the shorter substrate to form a nonproductive complex with the ribozyme, only substrates that contained an unpaired 5′-terminal cytosine were used for further experiments.

A minimal kinetic mechanism for intermolecular hairpin catalysis (Figure 2) includes substrate binding (k_1), cleavage (k_2), release of P1 and P2 cleavage products (k_3 and k_4), and the reverse steps of substrate dissociation (k_{-1}), ligation (k_{-2}), and product binding (k_{-3} and k_{-4}). Because cleavage

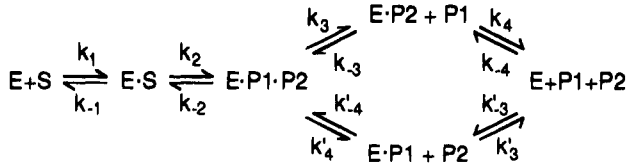

FIGURE 2: Minimal kinetic mechanism for intermolecular catalysis by the hairpin ribozyme.

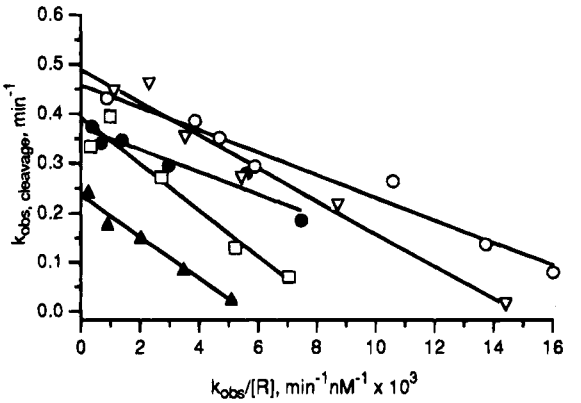

FIGURE 3: Kinetic parameters for hairpin cleavage. The ribozyme concentration dependence of $k_{obs,\ cleavage}$ is presented in Eadie–Hofstee plots for typical cleavage reactions with ribozyme in excess of substrate. Cleavage rate constants between 0.2 and 0.5 min^{-1} were determined from the *Y*-intercept, and K_M^S values between 20 and 50 nM were determined from the slope for R1-mediated cleavage of S1 (▲) and S4 (●) and R5-mediated cleavage of S6 (□), S7 (▽), and S8 (○). Values for all hairpin ribozyme–substrate pairs that are the average of three such determinations are presented in Table 1.

substrates differed greatly from their corresponding products in dissociation kinetics (below), no single ribozyme/substrate pair gave rate constants in the measurable range for every step in the kinetic mechanism. Therefore, complementary kinetic and equilibrium experiments were carried out with a series of substrates and products with a range of affinities for the ribozyme. In this way, rate and/or equilibrium constants were determined for each step in the mechanism, either directly or through calculation.

Kinetics of Substrate Cleavage. To determine kinetic parameters for cleavage reactions, k_2 and K_M^S, the appearance of [5′-^{32}P]P1 was measured over time in reactions that contained small amounts of [5′-^{32}P]substrate and several concentrations of ribozyme in excess of substrate. A complete reaction does not require product release because all substrate is expected to cleave during the first turnover when ribozyme is in excess. Furthermore, when ribozyme is in large excess over products, no ribozyme can form a ternary complex by rebinding both products after they dissociate. Consequently, unless both cleavage products remain associated with ribozyme long enough to undergo ligation, no ligation can occur and $k_{obs,\ cleavage}$ will reflect the rate-determining step in the cleavage reaction that precedes product release.

For all substrates shown in Figure 1B, cleavage rates increased linearly with increasing concentrations of ribozyme below 20 nM. At ribozyme concentrations above ~400 nM, cleavage rates approached a constant value of about 0.3 min^{-1}, indicating that saturation was reached. Values for K_M^S and the cleavage rate constant, k_2, were determined from plots of $k_{obs,\ cleavage}$ versus $k_{obs,\ cleavage}$/[R] (Figure 3). Cleavage rate constants ranged between 0.19 and 0.45 min^{-1} and K_M^S

Table 1: Kinetic Parameters for Cleavage and Ligation[a]

ribozyme	substrate	k_2[b] (min^{-1})	K_M^S[b] (nM)	k_2/K_M^S[c] ($nM^{-1}min^{-1}$)	$k_{cat,cleavage}$[d] (min^{-1})	K_M^S[d] (nM)	k_{-2}[e] (min^{-1})	K_M^{P1}[e] (μM)
R1	S1	0.19 ± 0.04	34 ± 8	0.0056	0.12 ± 0.05	31 ± 6		
R1	S2	0.30 ± 0.01	29 ± 2	0.010			1.1 ± 0.1	57 ± 44
R1	S3	0.23 ± 0.02	68 ± 10	0.0034				
R1	S4	0.39 ± 0.06	30 ± 4	0.013				
R5	S5	0.38 ± 0.05	30 ± 1	0.013	0.22 ± 0.02	43 ± 6		
R5	S6	0.39 ± 0.03	40 ± 7	0.0098			3.5 ± 0.9	3.3 ± 1.7
R5	S7	0.37 ± 0.09	21 ± 8	0.018				
R5	S8	0.45 ± 0.03	21 ± 2	0.021				

[a] Mean and range of values obtained from three or more determinations. [b] Values obtained from plots of k_{obs} versus $k_{obs}/[R]$ in ribozyme-excess reactions with ribozyme concentrations ranging from 0.001 to 2 μM and [5′-^{32}P]substrate concentrations less than 0.0001 μM. [c] Calculated from K_M^S and k_2 values determined from single-turnover, ribozyme-excess experiments. [d] Values obtained from plots of k_{obs} versus $k_{obs}/[S]$ in reactions with [5′-^{32}P]substrate concentrations ranging from 0.005 to 0.5 μM and ribozyme concentrations that were at least 10-fold lower. [e] Calculated from $k_{obs,\ ligation}$ in reactions with [R·P2] ranging from 0.005 to 30 μM and [5′-^{32}P]P1 at concentrations less than 0.001 μM, by computing the fit to $k_{obs,\ ligation} = k_{-2}([E{\cdot}P2]/([E{\cdot}P2] + K_M^{P1})) + k_2$, as described in the text.

values fell between 20 and 70 nM for all ribozyme/substrate pairs, regardless of substrate length or sequence (Table 1).

In reactions with ribozyme in excess of substrate, or in multiple-turnover reactions when product release is fast compared to earlier steps, K_M^S is related to elemental rate constants according to eq 1.

$$K_M^S = (k_{-1} + k_2)/k_1 \quad (1)$$

Therefore, when rate constants for substrate dissociation (k_{-1}) are small compared to cleavage rate constants (k_2), K_M^S values will not reflect the ratio of substrate dissociation and binding rate constants, k_{-1}/k_1 or K_d^S but instead will reflect the ratio of cleavage and substrate binding rate constants, k_2/k_1. The similarity of K_M^S values among ribozyme/substrate pairs that were expected to vary greatly in stability suggested that K_M^S was not equal to K_d^S for hairpin cleavage and that dissociation rate constants for all substrates were small compared to cleavage rate constants. For each of these substrates, in other words, virtually all substrate that bound ribozyme was cleaved before it could dissociate. By assuming that k_{-1} is small and that $K_M^S \cong k_2/k_1$, substrate binding rate constants, k_1, can be calculated from K_M^S and k_2, giving values on the order of 1×10^7 M^{-1} min^{-1} (Table 1).

For R1/S1 and R5/S5 hairpins, multiple-turnover cleavage kinetics were also assayed in reactions with several concentrations of substrate in 10-fold or greater excess over ribozyme concentrations. Cleavage rates were calculated from plots of [P]/[R] versus time during the initial phase of the reaction. K_M^S and k_{cat} values that were calculated from the substrate concentration dependence of cleavage rates during the single-turnover and multiple-turnover phases of the reactions agreed within 2-fold with k_2 and K_M^S values measured in ribozyme-excess experiments (Table 1). Since kinetic parameters were calculated from ratios of product and ribozyme concentrations in substrate-excess experiments, the similarity between cleavage rate constants and K_M^S values obtained from ribozyme-excess and substrate-excess reactions indicated that most of the RNA in ribozyme and substrate preparations was functional. Because substrate-excess reactions are more subject to errors in RNA concentration estimates, kinetic parameters obtained from ribozyme-excess experiments are likely to be more accurate.

Since multiple-turnover cleavage rate constants, k_{cat}, were not significantly slower than single-turnover rate constants, k_2, dissociation of S1−P1, S5−P1, and S1−P2, or S5−P2 could not be much slower than cleavage because cleavage products must be released from the ribozyme before the second turnover. To confirm this result, S1−P2 dissociation and S1 cleavage rates were compared by combining R1 with an excess, saturating concentration of S1−P2 before dilution into [5′-^{32}P]S1. Cleavage occurred at the same rate as in parallel reactions with no added S1−P2 (data not shown). Since S1−P2 must dissociate before [5′-^{32}P]S1 can bind and cleave in this experiment, the absence of an effect on cleavage rates of preincubation with S1−P2 showed that S1−P2 dissociation could be no slower than cleavage.

Kinetics of Product Ligation. Kinetic parameters were measured for ligation of S2−P2, the longest 3′-cleavage product, with S1−P1 or S5−P1 to form S2 or S6, respectively (Figure 4A). Ribozyme was first combined with a slight excess of S2−P2 at concentrations high enough to ensure that all ribozyme would form a binary complex with S2−P2. A small amount of [5′-^{32}P]S1−P1 or [5′-^{32}P]S5−P1 was added to the R·P2 complex to initiate the reaction, and the appearance of ligated substrate, [5′-^{32}P]S2 or [5′-^{32}P]S6, was measured over time.

The rate of ligation will be the product of the ligation rate constant, k_{-2}, and the concentration of the ternary complex containing the ribozyme and both cleavage products, or k_{-2}[E·P1·P2]. The concentration of ternary complex reflects K_M^{P1} and the concentration of the binary complex containing the ribozyme and P2, or [E·P2], as shown in eq 2. As

$$[E{\cdot}P1{\cdot}P2] = [E{\cdot}P2]/([E{\cdot}P2] + K_M^{P1}) \quad (2)$$

ligation proceeds, newly formed substrate will cleave at a rate that is the product of the cleavage rate constant and the concentration of the ribozyme−substrate complex, or k_2[E·S]. Because R1/S2 and R5/S6 complexes dissociate much more slowly than they cleave (below), newly formed substrate is expected to remain bound to ribozyme throughout the reaction so that [E·S] is virtually the same as $[S]_{total}$. Furthermore, because the R·P2 binary complex was in large excess over substrate, the fraction of ribozyme in the form of E·S was always very small, so $[E{\cdot}P2]_{total}$ remained virtually constant throughout the reaction. Therefore, the observed rate of appearance of ligated substrate, $k_{obs,\ ligation}$, reflects the approach to the equilibrium between ligation of products and cleavage of bound substrate according to eq 3,

$$k_{obs,\ ligation} = k_{-2}([E{\cdot}P2]/([E{\cdot}P2] + K_M^{P1})) + k_2 \quad (3)$$

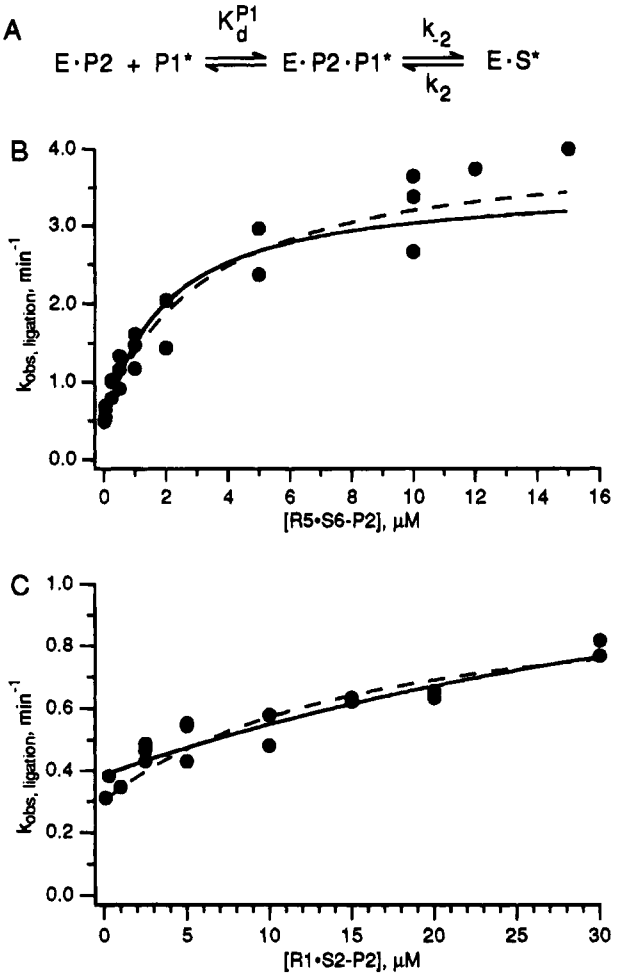

FIGURE 4: Kinetic parameters for ligation reactions. A, scheme of the reaction used to assay ligation kinetics. B, a preannealed complex of ribozyme, R5, and the 3′-cleavage product, S6−P2, at concentrations ranging from 0.05 to 15 μM, was combined with 1 nM or less of radioactive 5′-cleavage product, [5′-^{32}P]S5−P1, and the appearance of ligated substrate, [5′-^{32}P]S6, was monitored over time. Observed ligation rates, determined from exponential fits of the fraction of [5′-^{32}P]S6 versus time, are plotted as a function of R5·S6−P2 concentration. The solid line represents the best fit to $k_{obs, ligation} = k_{-2}([R5{\cdot}S6{-}P2]/([R5{\cdot}S6{-}P2] + K_M^{S5-P1})) + k_2$, as described in the text. The dashed line represents the best fit to the same equation but with the value of k_2 held constant at 0.4 min^{-1}. C, a preannealed complex of ribozyme, R1, and the 3′-cleavage product, S2−P2, at concentrations ranging from 0.05 to 30 μM, was combined with 1 nM or less of radioactive 5′-cleavage product, [5′-^{32}P]S1−P1, and the appearance of ligated substrate, [5′-^{32}P]S2, was monitored over time. Observed ligation rates, determined from exponential fits of the fraction of [5′-^{32}P]S2 versus time, are plotted as a function of R1·S2−P2 concentration. The solid line represents the best fit to $k_{obs, ligation} = k_{-2}([R1{\cdot}S2{-}P2]/([R1{\cdot}S2{-}P2] + K_M^{S1-P1})) + k_2$, as described in the text. The dashed line represents the best fit to the same equation but with the value of k_2 fixed at 0.3 min^{-1}.

where [E·P2] = [E]$_{total}$. In reactions monitoring ligation of S5−P1 and S6−P2 to form S6, computing the best fit to eq 3 for $k_{obs, ligation}$ as a function of R5·S6−P2 concentration gave a ligation rate constant, k_{-2}, of 3.5 min^{-1}, a K_M^{S5-P1} value of 3.3 μM, and a cleavage rate constant, k_2, of 0.6 min^{-1} (Figure 4B, Table 1). When k_2 was fixed at the independently determined cleavage rate constant of 0.4 min^{-1}, computed fits for K_M^{S5-P1} and k_{-2} changed little, giving values of 1.9 μM and 3.1 min^{-1}, respectively. As expected, [5′-^{32}P]S5−P1 containing 2′- or 3′-phosphate rather than 2′,3′-cyclic phosphate termini was not reactive. Purified [5′-^{32}P]S6 formed by ligation cleaved at the same rate and to the same extent as chemically synthesized [5′-^{32}P]S6, evidence that ligation occurred through a simple reversal of the cleavage reaction (data not shown).

Calculation of the internal equilibrium between ligation and cleavage, K_2, from the ratio of ligation and cleavage rate constants (eq 4), shows that, at saturating concentrations,

$$K_{eq(int)} = K_2 = k_{-2}/k_2 \quad (4)$$

ligation was favored over cleavage nearly 10-fold.

In a ribozyme-excess ligation reaction, K_M^{S5-P1} is related to the ligation rate constant, k_{-2}, the P1 dissociation rate constant, k_3, and the P1 binding rate constant, k_{-3}, according to eq 5,

$$K_M^{P1} = (k_3 + k_{-2})/k_{-3} \quad (5)$$

A lower limit of $\sim 1 \times 10^6$ M^{-1} min^{-1} can be calculated for the S5−P1 binding rate constant, k_{-3}, from the K_M^{S5-P1} value of 3.3 μM, the k_{-2} value of 3.5 min^{-1}, and the k_3 value of 0.22 min^{-1}, the lower limit on the rate constant for S5−P1 dissociation defined by the S5 multiple-turnover cleavage rate constant. Since K_d^{S5-P1}, which is k_3/k_{-3}, was the same as K_M^{S5-P1} (below), however, the S5−P1 dissociation rate constant, k_3, is probably large compared to the ligation rate constant, k_{-2}. If so, the S5−P1 binding rate constant would be higher than this lower limit.

R1-mediated ligation of S1−P1 and S2−P2 to form S2 could be measured only with subsaturating concentrations of the R1·S2−P2 complex because S1−P1 bound ribozyme with lower affinity than S5−P1 (below). Because $k_{obs, ligation}$ values varied less than 3-fold over the concentration range that could be assayed, kinetic parameters for R1-mediated ligation could only be approximated. The fit to eq 3 for the dependence of $k_{obs, ligation}$ of S1−P1 on the concentration of R1·S2−P2 gave a ligation rate constant of 1.1 min^{-1}, a cleavage rate constant of 0.4 min^{-1}, and a K_M^{S1-P1} value of 57 μM (Figure 4C, Table 1). When the fit was recalculated with a k_2 value fixed at the measured cleavage rate constant of 0.3 min^{-1}, the computed ligation rate constant and K_M^{S1-P1} values dropped to 0.7 min^{-1} and 15 μM, respectively, indicating that k_{-2} and K_M^{S1-P1} were not determined independently by the data for this ribozyme−substrate pair.

Product Binding and Dissociation Rate and Equilibrium Constants. Equilibrium dissociation constants for complexes between ribozymes and cleavage products were measured by determining the fraction of product bound as a function of ribozyme concentration using nondenaturing gel shift assays (Pyle et al., 1990; Fedor & Uhlenbeck, 1992). Because some complexes could not be detected following nondenaturing gel electrophoresis at 25 °C, presumably because they dissociated during the time required for sample loading and electrophoresis, binding reactions were equilibrated in solution at 25 °C and electrophoresis was carried out at 5 °C. For cases in which it was possible to quantitate an array of species with mobilities between those of free and bound ligand at 25 °C, assumed to reflect ligand that was bound in solution but that dissociated during electrophoresis, K_d values that were determined after electrophoresis at 5 and at 25 °C agreed within 5-fold (data not shown).

The K_d value of 3.8 μM that was measured for the R5·S5−P1 complex (Figure 5A) agreed well with the

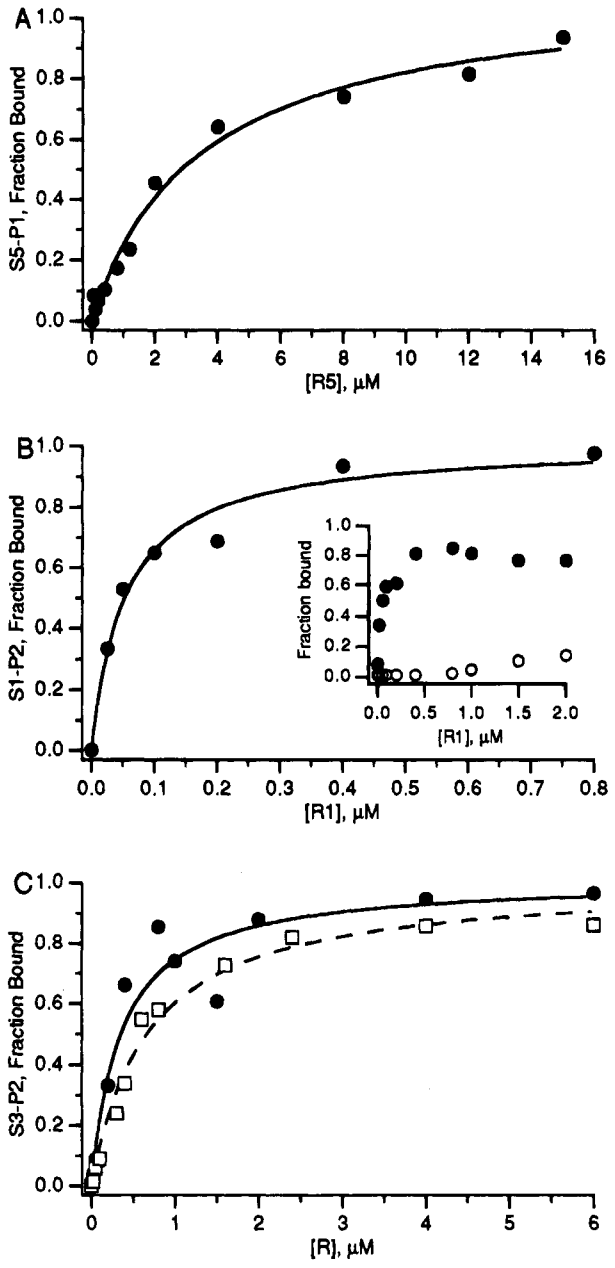

FIGURE 5: Determination of equilibrium dissociation constants for ribozyme−product complexes. The fraction of bound product, FB, is shown as a function of ribozyme concentration. Lines represent the best fits to the equation, FB = [R]/([R] + K_d^P). A, fraction of bound [5′-^{32}P]S5−P1 is plotted as a function of R5 concentration. The fit to a theoretical binding curve gave a K_d^{S5-P1} value of 3.8 μM. B, The fit to a theoretical binding curve (solid line) of the fraction of bound [5′-^{32}P]S1−P2 plotted as a function of R5 concentration (●) gave a K_d^{S1-P2} value of 68 nM. Inset, the fraction of [5′-^{32}P]S1−P2 migrating as fast (●) or slow (○) mobility species is shown as a function of R5 concentration. C, the fit to a theoretical binding curve (solid line) of the fraction of bound [3′-^{32}P]S3−P2 as a function of R1 concentration (●) gave a K_d^{S3-P2} value of 360 nM. The fit to a theoretical binding curve (dashed line) of the fraction of bound [5′-^{32}P]S3−P2 as a function of R5 concentration (□) gave a K_d^{S3-P2} value of 670 nM. The mean and range of K_d values obtained from three or more similar experiments were used to calculate ΔG values in Table 2.

K_M^{S5-P1} value of 3.3 μM that was determined from the concentration dependence of S5−P1 ligation (Figure 4B, Table 1). Since $K_M^{S5-P1} = (k_3 + k_{-2})/k_{-3}$, as shown in eq 5, and $K_d^{S5-P1} = k_3/k_{-3}$, the similarity between the K_d^{S5-P1} and K_M^{S5-P1} values supports the idea that K_M^{S5-P1} is the same as K_d^{S5-P1} and that the rate constant for S5−P1 dissociation, k_3, is fast relative to the ligation rate constant, k_{-2}. Furthermore, since K_M^{S5-P1} reflects the binding of S5−P1 to the R5·S6−P2 complex while K_d^{S5-P1} was measured in the absence of P2, the similarity between K_M^{S5-P1} and K_d^{S5-P1} indicated that any effect of one cleavage product on binding of the other was small.

In experiments designed to measure the S5−P1 binding rate constant, k_{-3}, by pulse−chase nondenaturing gel electrophoresis (Hertel et al., 1994), [5′-^{32}P]S5−P1 was combined with various concentrations of R5 and samples were applied to nondenaturing gels after various times to measure complex formation. At the high nanomolar concentrations required to detect the R5·S5−P1 complex, however, S5−P1 binding was complete at the earliest time points (data not shown). Although S5−P1 binding rates were too fast to measure, these results were consistent with the lower limit of 1×10^6 M^{-1} min^{-1} for the S5−P1 binding rate constant that was calculated from K_M^{S5-P1} and k_{-2} values (above, eq 5, Table 1).

Pulse−chase nondenaturing gel experiments were also attempted to measure S5−P1 dissociation rates. An R5·[5′-^{32}P]S5−P1 complex, which was formed with a high concentration of R5, was diluted to prevent rebinding of any RNA that dissociated and then fractionated on nondenaturing gels after various times to monitor the disappearance of the complex. No complex was detected at the earliest time points after dilution (data not shown), indicating that S5−P1 dissociation was too fast to measure. Although S5−P1 dissociation rates could not be measured directly, this result was consistent with the rapid S5−P1 dissociation rates expected from cleavage, ligation, and equilibrium binding experiments, above.

No complex between R1 and S1−P1 could be detected on nondenaturing gels at any temperature or any concentration of R1, presumably because the complex dissociated rapidly during electrophoresis. While a K_d value for the R1·S1−P1 complex could not be determined with this assay, the apparent instability of the complex during electrophoresis was consistent with the high K_M^{S1-P1} value inferred from the concentration dependence of S1−P1 ligation kinetics, above. Specifically, if K_d^{S1-P1} were equal to the K_M^{S1-P1} value of 57 μM, and if the S1−P1 binding rate constant was $\sim 1 \times 10^7$ M^{-1} min^{-1}, similar to values measured for other substrates and products, then the R1·S1−P1 complex would dissociate with a $t_{1/2}$ of less than 0.1 s.

Nondenaturing gel fractionation of equilibrium binding reactions with ribozymes and radioactive 3′-cleavage products revealed two ribozyme-dependent complexes that migrated with different mobilities and appeared over distinct ranges of ribozyme concentrations (Figure 5B). In binding reactions with [^{32}P]S1−P2 and ribozyme ranging in concentration from 25 to 2000 nM, for example, virtually all [^{32}P]S1−P2 shifted into a rapidly migrating complex at ribozyme concentrations below 1000 nM (Figure 5B) while a lower mobility complex was detected at ribozyme concentrations of 1000 nM and higher (Figure 5B, inset). Similarly, complete binding of [^{32}P]S3−P2 in a rapidly migrating complex occurred at ribozyme concentrations below 4000 nM (Figure 5C) while a slowly migrating species was detected at concentrations of 4000 nM and higher (data not shown). No analogous species had been detected in S5−P1 binding reactions, above. At concentrations above 1000 nM, nondenaturing gel electrophoresis of [5′-^{32}P]R1 in the

absence of any product RNA gave rise to a species with an electrophoretic mobility that was indistinguishable from the slowly migrating complex detected in [^{32}P]P2 binding reactions (data not shown). Thus, the low-mobility species appeared to represent a ribozyme aggregate that was able to bind P2. At a concentration of 30 μM, about 13% of R1 migrated as an aggregate (data not shown). An equilibrium dissociation constant of ~150 μM can be estimated by assuming that the low-mobility species represented a ribozyme dimer and that dimer formation would proceed to completion at high concentrations. The low-mobility species might correspond to a ribozyme complex that was previously identified in cross-linking experiments (Butcher & Burke, 1994a). Since no more than 13% of the ribozyme appeared in the low-mobility species at the highest concentrations used for kinetics and equilibrium binding experiments, ribozyme aggregation was not likely to interfere with interpretation of these experiments.

Equilibrium dissociation constants were calculated for the rapidly migrating complexes of S1−P2 and S3−P2 from the fraction bound at ribozyme concentrations below those required for detection of the low-mobility species. Similar K_d values of 89 and 80 nM were determined for complexes containing S1−P2 and R1 or R5 ribozymes, respectively (shown for the R5·S1−P2 complex in Figure 5B). K_d values for complexes between S3−P2 and R1 or R5 ribozymes averaged 590 and 510 nM, respectively (shown for one R1·S3−P2 experiment in Figure 5C). The 6-fold decrease in stability of R·S3−P2 compared to R·S1−P2 complexes was consistent with the change in binding energy expected from the loss of an A·U base pair in the shorter helix formed by S3−P2. No significant difference in stability was detected between complexes containing [5′-^{32}P]P2 with a 5′-monophosphate terminus and [3′-^{32}P]P2 with the appropriate 5′-hydroxyl terminus (shown for S3−P2 in Figure 5C). The affinities of ribozyme complexes with the longest and shortest 3′-cleavage products, S2−P2 and S4−P2, were too high or too low, respectively, to be assayed by nondenaturing gel electrophoresis.

Rate constants for binding of S2−P2 to R1 and R5 ribozymes, k_{-4}, were measured by pulse−chase nondenaturing gel electrophoresis, as described by Hertel et al. (1994). A small amount of [^{32}P]S2−P2 was combined with several concentrations of ribozyme, and the fraction of ribozyme-bound [^{32}P]S2−P2 was monitored after various times using nondenaturing gel electrophoresis. Values for $k_{obs,\ binding}$ for each ribozyme concentration were obtained from plots of ln(fraction unbound) versus time (Figure 6A, inset). The observed rate of complex formation reflects the rate of approach to equilibrium, which is the sum of the binding and dissociation rates as shown in eq 6. Rate constants for

$$k_{obs,\ binding} = k_{-4}[E] + k_4 \quad (6)$$

S2−P2 binding to R1 and R5 of 2 × 10^8 M^{-1} min^{-1} were obtained from the slope of plots of $k_{obs,\ binding}$ versus ribozyme concentration (Table 2, shown for R5 in Figure 6A). The Y-intercepts were near zero, indicating a very low rate constant for S2−P2 dissociation. Binding rate constants for [3′-^{32}P]S2−P2 and [5′-^{32}P]S2−P2 were indistinguishable (data not shown), indicating that binding was unaffected by the presence or absence of phosphate at the 5′-terminus.

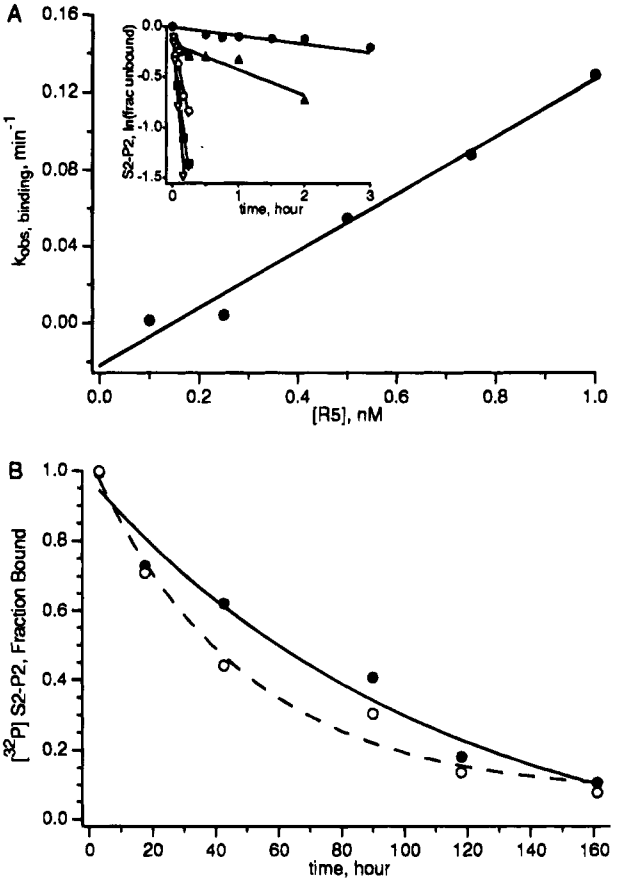

FIGURE 6: Product binding and dissociation rate constants, k_{-4} and k_4. A, binding reactions containing small amounts of [^{32}P]S2−P2, and different concentrations of R5 were fractionated by nondenaturing gel electrophoresis after various times. Inset, observed binding rates were calculated from plots of ln(fraction unbound) versus time at R5 concentrations of 0.01 (●), 0.25 (▲), 0.5 (○), 0.75 (■), and 1 nM (▽). The slope of the plot of $k_{obs,\ binding}$ versus [R5] gave a rate constant for S2−P2 binding, k_{-4}, of 1.5 × 10^8 M^{-1} min^{-1}. B, a small amount of [^{32}P]S2−P2 was combined with 20 nM R1 or R5 for an initial binding period and diluted into a 200-fold excess of nonradioactive S2−P2, and the disappearance of the R·[^{32}P]S2−P2 complex was monitored over time. Dissociation rate constants, k_4, of 1.5 × 10^{-4} and 3.5 × 10^{-4} min^{-1} were obtained from exponential fits to plots of the fraction of bound [^{32}P]S2−P2 versus time for R1 (solid line) and R5 (dashed line), respectively. The mean and range of values obtained from three or more similar experiments appear in Table 2.

Pulse−chase nondenaturing gel electrophoresis experiments were designed to measure the rate constant for dissociation of S1−P2 and S2−P2, k_4, by monitoring the decay of a complex formed with a small amount of [^{32}P]P2 and a saturating concentration of ribozyme after dilution to prevent rebinding of any dissociated [^{32}P]P2. In experiments with S1−P2, however, almost no complex could be detected 10 s after dilution, indicating that S1−P2 dissociation was too fast to be determined using this assay. By assuming a rate constant for S1−P2 binding of 2 × 10^8 M^{-1} min^{-1}, which is the binding rate constant that was measured for S2−P2, a dissociation rate constant greater than 15 min^{-1} can be calculated for S1−P2 based on the K_d^{S1-P2} value of 89 nM. An R·S1−P2 complex with a $t_{1/2}$ less than 3 s would be expected to disappear rapidly upon dilution. A rapid S1−P2 dissociation rate constant was also consistent with the similarity between single- and multiple-turnover S1 and S5 cleavage rate constants, above, which indicated that S1−P2 dissociation was faster or on the same order as cleavage.

Table 2: Binding and Dissociation Rates and Binding Energies for Cleavage Products[a]

complex	$\Delta G_{25°C,measured}$[b] (kcal/mol)	$\Delta G_{25°C,helix}$[e] (kcal/mol)	k_{off} (min^{-1})	k_{on} ($nM^{-1}\,min^{-1}$)
R5·S5−P1 ⇌ R5 + S5−P1	−7.4 ± 0.2[c]	−8.2	≥0.22[f]	
R1·S1−P2 ⇌ R1 + S1−P2	−9.6 ± 0.2[c]	−7.1	≥0.12[f]	
R5·S1−P2 ⇌ R5 + S1−P2	−9.6 ± 0.2[c]	−7.1	≥0.22[f]	
R1·S2−P2 ⇌ R1 + S2−P2	−15.5± 0.6[d]	−14.0	0.0009 ± 0.0005[g]	0.22 ± 0.08[g]
R5·S2−P2 ⇌ R5 + S2−P2	−15.5± 0.5[d]	−14.0	0.0007 ± 0.0003[g]	0.19 ± 0.06[g]
R1·S3−P2 ⇌ R1 + S3−P2	−8.5 ± 0.2[c]	−6.0		
R5·S3−P2 ⇌ R5 + S3−P2	−8.5 ± 0.2[c]	−6.0		

[a] Mean and range of values obtained from two or more experiments. [b] Calculations based on $\Delta G = -RT \ln(1/K_d)$, where R is the gas constant and T is the temperature in degrees Kelvin. [c] Calculation based on the mean and range of K_d values obtained from two or more nondenaturing gel shift assays, as described in text. [d] Calculation based on the K_d value obtained from the ratio of measured dissociation and binding rate constants. [e] Calculation based on empirically determined free energy parameters for base-paired RNA helices (Turner et al., 1988). [f] Lower limit determined from multiple-turnover cleavage rates as described in the text. [g] Determined from pulse−chase nondenaturing gel shift assays as described in the text.

In contrast to the instability of R·S1−P2 complexes, similar pulse−chase nondenaturing gel shift experiments with S2−P2 showed that a significant fraction of S2−P2 remained ribozyme-bound after 6 days. Although RNA degradation over this time period limited the accuracy of this measurement, rate constants of 0.0009 and 0.0007 min^{-1} for dissociation of S2−P2 from R1 and R5, respectively, were estimated from exponential fits to the fraction of bound S2−P2 versus time (Figure 6B). A K_d^{S2-P2} value of $\sim 4 \times 10^{-12}$ M can be calculated from the ratio of S2−P2 dissociation and binding rate constants, k_4 and k_{-4} (Table 2). The decrease of more than 10^4-fold in the K_d^{S2-P2} value compared to the K_d^{S1-P2} value that was measured through equilibrium nondenaturing gel electrophoresis (above) was consistent with the change in binding energy expected from the additional base pairs in the helix formed by S2−P2.

Substrate Binding and Dissociation Rate and Equilibrium Constants. Rate constants for substrate dissociation were assayed using two types of partitioning experiments designed to compare dissociation rates to cleavage rates, which gave strikingly different results. In the first type of experiment (Figure 7A), a small amount of [5′-^{32}P]substrate was incubated with a high concentration of ribozyme for an initial binding period, t_1. Binding was expected to be complete by the end of t_1 since t_1 was more than 10 times longer than the $t_{1/2}$ for the binding reaction calculated from ribozyme concentrations and substrate binding rate constants. The binding reaction was then diluted to prevent rebinding of any dissociated substrate, and the appearance of cleavage products was measured during a chase period, t_2. For substrates S1, S2, S4, and S6, approximately half of the substrate that was measured at the end of the binding reaction remained uncleaved at the end of the chase period, suggesting that about half of each substrate escaped cleavage by dissociating during t_2 (shown for S4 in Figure 7B). Since each substrate appeared to partition more or less equally between cleavage and dissociation, this result suggested that cleavage and dissociation rates were about the same.

The apparent similarity in dissociation rates among substrates that were expected to bind ribozyme with very different affinities led us to consider experimental artifacts that could account for these results. Any fraction of substrate that failed to bind ribozyme during t_1 would remain intact during the subsequent chase and lead to an overestimation of k_{-1}, as discussed by Fedor and Uhlenbeck (1992). Variation in binding times from 1 to 4 min had no effect on substrate dissociation rate measurements, suggesting that the binding reaction was complete during t_1 since binding is

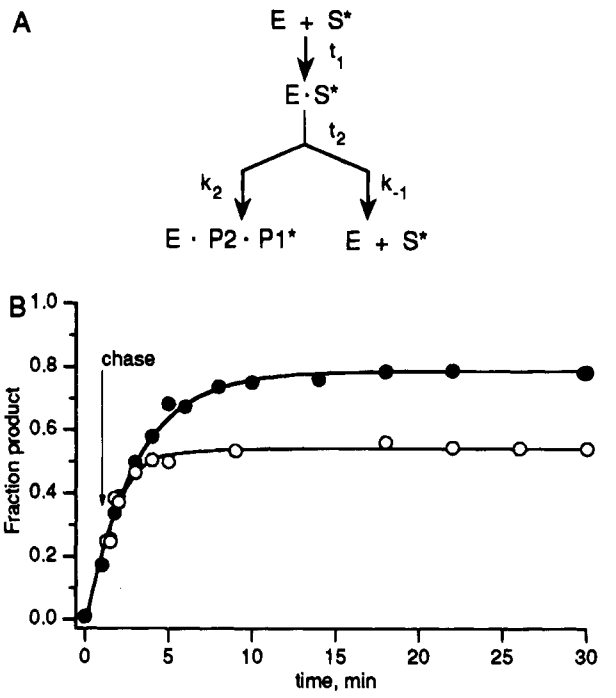

FIGURE 7: Determination of substrate dissociation rate constants, k_{-1}, from the partitioning between cleavage and dissociation of ribozyme−substrate complexes formed in a substrate binding reaction. A, reaction scheme used to monitor the decay of an R1·-[^{32}P]S4 complex, formed in a binding reaction during t_1, as it partitioned between cleavage and dissociation during t_2. B, the fraction of substrate converted to product is shown for a reaction in which 1.0 μM R1 was combined with a trace amount of [5′-^{32}P]S4. After 75 s, the reaction was diluted into 10 mL of 50 mM Tris-HCl, pH 7.5, 10 mM $MgCl_2$ (○) or allowed to proceed without dilution (●). In the control reaction, 24% of [5′-^{32}P]S4 was cleaved at 75 s, when the chase reaction was initiated, and 79% was cleaved by the end of the control reaction; 54% of the [5′-^{32}P]S4 that was intact at end of t_1 was cleaved by the end of t_2.

expected to increase with time. Nonetheless, a fraction of substrate might adopt a conformation that failed to bind during t_1 yet subsequently exchanged into a reactive conformation over the course of the control reaction. Any substrate that bound ribozyme and cleaved in the control reaction after the chase was initiated would result in an artifactually high extent of cleavage in the control reaction, relative to the chase, and overestimation of the substrate dissociation rate. Although no substrate conformational heterogeneity was detected on nondenaturing gels at these substrate concentrations, exchange between reactive and unreactive conformations that occurred on a time scale of minutes would likely escape detection.

In an attempt to disrupt any structures that might interfere with complete substrate binding, a preannealing step was incorporated into the binding phase of partitioning experiments with S1 and S4. R1 and [5′-^{32}P]S were combined in 50 mM Tris-HCl, pH 7.5, incubated for 1 min at 95 °C, centrifuged briefly to pellet condensate, and then incubated for several minutes at 25 °C. Control and chase reactions were initiated by adding $MgCl_2$. Cleavage rates and extents measured in control and chase reactions were the same regardless of whether ribozyme and substrate had been preannealed, indicating that preannealing did not increase the total fraction of substrate bound (data not shown).

A second type of experiment was designed to circumvent potential artifacts that could arise from incomplete or aberrant substrate binding (Figure 8A). Instead of generating the ribozyme−substrate complex in a binding reaction, the complex was formed by ribozyme-mediated ligation of [5′-^{32}P]P1 and P2. This method ensured that all [^{32}P]substrate was bound initially in a functional ribozyme complex. After the ligation reaction was diluted to prevent further ligation or rebinding of any dissociated substrate, substrate cleavage was monitored over time. Virtually no [^{32}P]substrate was detected in control experiments in which [5′-^{32}P]P1 was diluted into the chase solution before R·P2 was added, confirming that chase conditions allowed no further ligation. Similarly, no cleavage products were detected when [5′-^{32}P]S was diluted into the chase solution before R·P2 was added, evidence that chase conditions did not allow substrate binding. The partitioning between cleavage and dissociation of ribozyme−substrate complexes that formed in ligation reactions contrasted sharply with the partitioning of complexes that formed in binding reactions (see above). For each of the eight substrates, virtually all substrate that formed during the ligation reaction went on to cleave during the subsequent chase (shown for S4 in Figure 8B), indicating that all functional ribozyme−substrate complexes dissociated much more slowly than they cleaved.

In an effort to detect dissociation of the smallest substrates that were expected to have the lowest affinity for ribozyme, the ligation−chase partitioning experiment was modified by adjusting the pH of the chase solution to 5.5 instead of 7.5. Because cleavage was slower at pH 5.5 than at pH 7.5 (L. A. Sultzman, L. A. Hegg, and M. J. Fedor, unpublished data), reducing the pH of the chase solution allowed a longer time for substrate to dissociate before cleavage was complete. To maximize the yield of [^{32}P]substrate during the initial ligation phase, ligation reactions were carried at 4 °C instead of at 25 °C and with very high concentrations of ribozyme and P2. Even at low pH, virtually all S3, S7, and S8 continued to cleave completely during the chase, indicating that dissociation of these substrates remained much slower than cleavage (data not shown). However, about 11% of the S4 that formed during the ligation phase remained uncleaved at the end of the chase period, evidence that a small fraction of the substrate that was expected to bind ribozyme with the lowest affinity had dissociated during the chase (Figure 8C). The rate constant for S4 dissociation, k_{-1}, was calculated by comparing the extents and rates of cleavage in chase reactions to control reactions without the chase as described previously (Fedor & Uhlenbeck, 1992) and as summarized below.

The fraction of the substrate that cleaves during the chase will be proportional to the cleavage and substrate dissociation

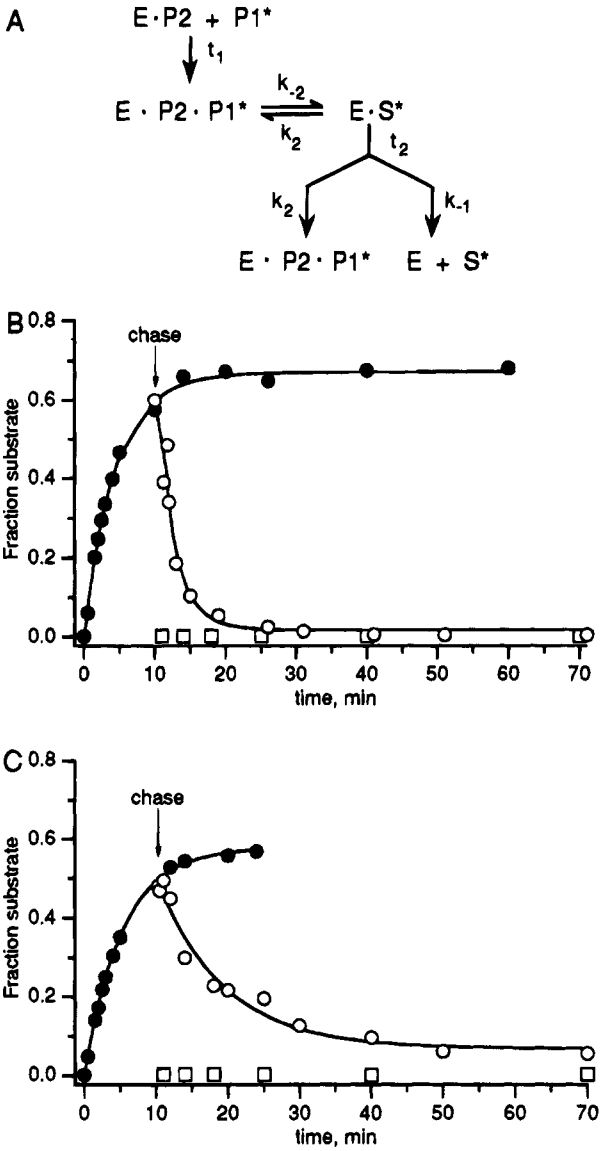

FIGURE 8: Determination of substrate dissociation rate constants, k_{-1}, from the partitioning between cleavage and dissociation of ribozyme−substrate complexes formed in a ligation reaction. A, reaction scheme used to monitor the decay of a R1·[^{32}P]S4 complex, formed in a ligation reaction during t_1, as it partitioned between cleavage and dissociation during t_2. B, a trace amount of [5′-^{32}P]-S1−P1 was combined with 30 μM R1·S4−P2 complex and underwent ligation for 10 min at 4 °C. The ligation reaction was then diluted into 10 mL of 50 mM Tris-HCl, pH 7.5, 10 mM $MgCl_2$ at 25 °C (○) or proceeded without dilution (●). Virtually no [5′-^{32}P]S4 that formed during t_1 remained uncleaved at the end of t_2. When [5′-^{32}P]P1 was diluted into the chase solution before the R1·-S4−P2 complex was added, less than 1% was converted to [5′-^{32}P]S4 by the end of t_2 (□). C, the same experiment shown in panel B was carried out except that the chase buffer was 50 mM MES, pH 5.5, 10 mM $MgCl_2$; 11% of the [5′-^{32}P]S4 that formed during t_1 remained uncleaved at the end of t_2 (○). Less than 1% of [5′-^{32}P]P1 that was diluted into the chase solution before the R1·S4−P2 complex was added was ligated by the end of t_2 (□).

constants according to eq 7,

$$[P]/([P] + [S]) = k_2/(k_2 + k_{-1}) \quad (7)$$

where P and S are radioactive product and substrate present at the end of t_2 after correction for the amount of substrate formed during t_1. Furthermore, since E·S decays through cleavage and dissociation, the chased reaction is completed

sooner than the control reaction, and the observed cleavage rate during the chase period, $k_{obs,\ chase}$, will be the sum of cleavage (k_2) and dissociation (k_{-1}) rate constants as shown in eq 8,

$$k_{obs,\ chase} = k_2 + k_{-1} \quad (8)$$

with the cleavage rate constant, k_2, measured in a control reaction at pH 5.5 and $k_{obs,\ chase}$ measured during the chase period. For S4, k_{-1} values calculated using eq 7 or 8 varied less than 2-fold, with an average value of 0.01 min^{-1}. A K_d value of 0.8 nM at pH 5.5 can be calculated for the R1·S4 complex from the ratio of substrate dissociation and binding rate constants.

DISCUSSION

Now that rate and equilibrium constants have been measured or calculated for individual steps in a minimal hairpin ribozyme kinetic mechanism, the hairpin mechanism can be compared to kinetic mechanisms of other ribozyme families to identify features which are common, unique to the hairpin, or shared by the hairpin with some, but not all, catalytic RNAs.

Rate Constant for Hairpin Cleavage. Eight hairpin ribozyme/substrate pairs that differed in the length and sequences of their intermolecular helices cleaved with virtually identical single-turnover kinetics with cleavage rate constants between 0.2 and 0.4 min^{-1} and K_M^S values between 20 and 70 nM. Cleavage rates ranging from 0.06 to 7.1 min^{-1} have been reported for similar ribozymes derived from the hairpin domain of (−)sTRSV (Hampel & Tritz, 1989; Feldstein et al., 1990; Hampel et al., 1990; Chowrira & Burke, 1991; Sekiguchi et al., 1991; Chowrira et al., 1993; Komatsu et al., 1993; Grasby et al., 1995). A number of factors might account for these differences. Variable kinetics could reflect the use of different temperatures and buffers, although reported rates vary more than expected from the shallow dependence of hairpin cleavage on pH and divalent ion concentration (Hampel & Tritz, 1989; Chowrira et al., 1993; L. A. Sultzman, L. A. Hegg, and M. J. Fedor, unpublished data). Alternatively, reactions carried out under different conditions might have different rate-determining steps. At low concentrations, for instance, substrate binding rather than cleavage will be rate-determining. Under the temperature and buffer conditions used here, cleavage was faster than substrate binding only at concentrations below 30 nM, when $k_1[E] < k_2$. Similarly, multiple-turnover reactions with substrate in excess could be limited by slow release of products, while single-turnover rates in reactions with ribozyme in excess reflect events that precede product release. However, previously characterized hairpin substrates were similar in sequence to S1, a substrate for which product dissociation rates were not significantly slower than cleavage rates at 25 °C. Slow product release would likely limit cleavage rates in multiple-turnover reactions at lower temperatures or in reactions with hairpin sequences that form more stable ribozyme−product complexes. Accumulation of a ternary complex containing the ribozyme and both products would promote ligation and reduce apparent cleavage rates. Although S1−P1, a 5′-cleavage product with the (−)sTRSV sequence, appeared to bind ribozyme with an affinity in the micromolar range and dissociate rapidly, competing ligation could reduce apparent cleavage rates in reactions that generate high concentrations of products or with hairpin sequences that form more stable intermolecular helices. Finally, small RNAs can adopt stable structures that interfere with ribozyme−substrate complex formation (Fedor & Uhlenbeck, 1990). Since small sequence changes in hairpin substrates had dramatic effects on the propensity to aggregate or to bind ribozyme nonproductively, structural heterogeneity of ribozymes, substrates, or complexes between the two might well contribute to variation in cleavage kinetics.

The hairpin cleavage rate constant of 0.3 min^{-1} is similar to the rate constant of 1 min^{-1} measured for hammerhead cleavage under identical conditions and represents ~10^5-fold acceleration over uncatalyzed phosphodiester hydrolysis (Fedor & Uhlenbeck, 1990, 1992; Hertel et al., 1993). The hammerhead cleavage rate constant is believed to reflect the rate of the base-catalyzed chemical conversion of substrates to products, in part because rates increase with increasing hydroxide ion concentration (Dahm et al., 1993; Hertel & Uhlenbeck, 1995). In contrast, hairpin cleavage rates changed little between pH 5.5 and 8 (Hampel & Tritz, 1989), suggesting that the hairpin and hammerhead chemical mechanisms are different or that a step other than catalytic chemistry is rate-determining for hairpin cleavage. While no evidence presented here distinguishes between these possibilities, several potential determinants of hairpin cleavage rates can be excluded. The cleavage rate constant would reflect a balance between substrate cleavage and product ligation, for example, if cleavage products remained associated with the ribozyme long enough to undergo ligation. However, sequence changes that stabilized the P1 and P2 helices did not decrease cleavage rate constants. Dissociation rates for RNA duplexes normally decrease with increasing stability (Pörschke & Eigen, 1971; Craig et al., 1971; Pörschke et al., 1973; Ravetch et al., 1974). Therefore, the absence of an effect of changes in P1 or P2 helix stability on cleavage rate constants suggests that, for each hairpin ribozyme−substrate pair, dissociation of one or both cleavage products was always faster than ligation. Another potential determinant of cleavage rates was the rate or extent of secondary structure formation. Specifically, if saturation of ribozyme with substrate occurred through formation of just one of the two intermolecular helices and incomplete formation of the second helix limited the amount of catalytically proficient complex, then changes that stabilized the second helix would stimulate cleavage rates by shifting the equilibrium toward complete secondary structure formation. However, changes in the P1 and P2 helices that were expected to enhance their stability by 2−8 kcal/mol did not stimulate cleavage, so cleavage rate constants did not appear to reflect an equilibrium in P1 or P2 helix formation. Furthermore, cleavage that followed substrate binding and cleavage of substrate formed by ribozyme-mediated ligation of P1 and P2 occurred at virtually identical rates. Because cleavage rates were independent of the path by which the ribozyme−substrate complex formed, the reaction pathway can include no more than one stable ribozyme-bound intermediate.

Ligation Kinetics and the Internal Equilibrium between Cleavage and Ligation. The internal equilibrium between cleavage and ligation was previously measured for an intramolecular reaction of a hairpin configuration in which the P1 and P2 sequences were covalently joined to the

ribozyme by way of an oligocytidine linker and a hairpin loop, respectively (Feldstein & Bruening, 1993). Although cleavage and ligation rate constants for the intramolecular reaction appeared to be significantly slower than those measured here, circles predominated over linear forms at temperatures below 37 °C while linear forms were favored at higher temperatures. A ratio of cleavage and ligation products near 1 was also observed in reactions with the entire (−)sTRSV RNA (Buzayan et al., 1986b) and with a bimolecular hairpin configuration in which P1 was covalently joined to the ribozyme and P2 RNA was supplied in *trans* (Berzal-Herranz et al., 1992; Chowrira et al., 1993a). Comparison of different hairpin configurations requires caution, however, because the ratio of cleavage and ligation products at equilibrium might reflect different steps in the kinetic mechanism. Specifically, the extent of P1 helix formation might be different for a ligation reaction in which both cleavage products are supplied in *trans* compared to a reaction in which the P1 RNA is connected to the ribozyme through a linker because the constraint on linker conformation associated with P1 helix formation will be accompanied by an unfavorable entropy. At saturating concentrations, R5 hairpin-catalyzed ligation was about 10-fold faster than cleavage. Thus, in contrast to the hammerhead which catalyzes ligation at the 400-fold slower rate of 0.008 min^{-1} and favors cleavage over ligation ~130-fold under the same conditions (Hertel et al., 1994), the hairpin ribozyme is a more proficient ligase than it is a nuclease.

A priori, the internal equilibrium for the transesterification reaction could favor ligation or cleavage. In the hammerhead reaction, a favorable enthalpy for ligation appears to be overwhelmed by a strongly unfavorable entropy (Hertel & Uhlenbeck, 1995). While no net change in the number of covalent bonds occurs to drive the reaction in either direction, relief of strain in the 2′,3′-cylic phosphate upon 3′,5′-phosphodiester formation (Gerlt et al., 1975) is expected to contribute a favorable enthalpy for ligation while an entropic advantage in forming two products from one substrate is expected to promote cleavage. The entropic barrier to hammerhead ligation could be explained by differences in solvation or divalent ion binding between hammerhead E·S and E·P1·P2 complexes or it could reflect the ordering required to position reactive groups for ligation (Hertel et al., 1994; Hertel & Uhlenbeck, 1995). According to the latter model, the propensity of the hairpin ribozyme to catalyze ligation could indicate that hairpin E·S and E·P1·P2 complexes are both "rigid", while conversion of a "rigid" hammerhead E·S complex into a "floppy" E·P1·P2 complex upon cleavage results in a significant entropy gain (Hertel et al., 1994). The similar binding energetics of hairpin E·S and E·P1·P2 complexes are consistent with this view, as is discussed below.

Substrate and Product Binding Energetics. The stability of ribozyme complexes with cleavage products and substrates can be compared to the stability of simple RNA duplexes with the same sequences using calculations based on empirically determined free energy parameters (Turner et al., 1988). This comparison provides a gauge for determining whether hydrogen bonding and stacking energies within the helices can account for the observed binding energy or whether extrahelical stabilizing or destabilizing interactions must be invoked. In the case of the *Tetrahymena* ribozyme, for example, a discrepancy of ~6 kcal/mol between calculated and measured stabilities of the helix formed by base pairing between the substrate and the ribozyme led to the identification of tertiary interactions between the substrate binding helix and the ribozyme core (Sullivan & Cech, 1985; Sugimoto et al., 1988, 1989; Pyle et al., 1990, 1992; Herschlag & Cech, 1990; Pyle & Cech, 1991, 1992; Bevilacqua & Turner, 1991; Strobel & Cech, 1993). In contrast, measured binding energies provided no evidence for stabilizing interactions between the hammerhead ribozymes and substrates or products beyond those implicit in the secondary structure (Fedor & Uhlenbeck, 1992; Hertel et al., 1994).

The R5 complex with S5−P1, with a K_d value of 3.8 μM, was less stable than expected for a simple RNA duplex with the same sequence by ~0.8 kcal/mol (Table 2). This relatively minor difference might reflect imprecision in the free energy calculation for the helix or inaccuracy in the K_d^{S5-P1} measurement, although the K_d^{S5-P1} value obtained from nondenaturing gel shift assays agreed well with the K_M^{S5-P1} value obtained from ligation reactions. While the affinity between R1 and S1−P1 was too weak to be measured directly, the high K_M^{S1-P1} value inferred from the concentration dependence of S1−P1 ligation was consistent with the reduction in stability expected for the substitution of the A_{-3}·U_{12} base pair in the S1−P1 helix for the G_{-3}·C_{12} base pair in the S5−P1 helix. The rapid binding and dissociation kinetics that precluded direct measurements of k_3 and k_{-3} were nonetheless consistent with the behavior expected for an RNA duplex analogous to the P1 helix (Pörschke & Eigen, 1971; Craig et al., 1971; Pörschke et al., 1973; Ravetch et al., 1974). Thus, the P1 helix did not deviate in any detectable way from the kinetics expected for a short RNA duplex, and stacking and hydrogen-bonding interactions within the P1 helix appear to account for most of the observed binding energy. The similarity between measured and calculated affinities does not, of course, preclude participation of the P1 helix in extrahelical interactions that produce no net energy gain or loss.

In contrast to ribozyme complexes with 5′-cleavage products, ribozymes bound 3′-cleavage products with affinities that were ~2.5 kcal/mol stronger than expected for simple helices with the same sequences (Table 2). The measured K_d^{S1-P2} and K_d^{S3-P2} values were 80-fold lower than values calculated for simple helices with the same sequences. Because ribozyme complexes with long and short P2 helices varied by more than 8 kcal/mol in binding energy and yet showed similar increases in stability relative to the binding energies calculated for analogous helices, the stability of any hairpin ribozyme−P2 complex can likely be predicted by combining the change in free energy calculated for helix formation with a constant extrahelical binding energy of −2.5 kcal/mol, or $\Delta G_{25\ ^\circ C}^{E\cdot P2} = \Delta G_{25\ ^\circ C}^{P2\ helix} - 2.5$ kcal/mol.

Extrahelical binding energy in ribozyme−P2 complexes could arise from stabilizing interactions within the helix−loop−helix domain that contains the reactive phosphodiester or between the two helix-loop-helix domains. A number of mutations and modifications of base and ribose functional groups have been found to interfere with hairpin catalysis (Hampel et al., 1990; Chowrira & Burke, 1991; Sekiguchi et al., 1991; Berzal-Herranz et al., 1992; Joseph et al., 1993; Chowrira et al., 1993; Grasby et al., 1995), and any of these might affect catalysis by eliminating a tertiary interaction. Butcher and Burke (1994b) proposed that G_8, located within

the symmetrical loop that contains the reactive phosphodiester (Figure 1A), forms a tertiary contact across the loop because the guanine of G_8 was susceptible to chemical modification in the absence but not the presence of P2 and mutation of G_8 reduced catalytic efficiency (Berzal-Herranz et al., 1993). Consistent with this proposal, substitution of N^7-deazaguanosine for G_8 was found to increase K_M and decrease k_{cat} for hairpin cleavage (Grasby et al., 1995). Thermodynamic characterization of a series of 4-nucleotide symmetrical loops showed contributions to helix stability ranging from +3.0 to −4.8 kcal/mol with enhanced stability, characteristic of loop nucleotides engaged in hydrogen bonding (Wu et al., 1995) so an extrahelical contribution of −2.5 kcal/mol to the stability of the R·P2 complex is consistent with a hydrogen-bonding interaction across the bulge. By analogy to the *Tetrahymena* ribozyme, in which interactions between the ribozyme and 2′-hydroxyls in the substrate-binding helix contribute −6 kcal /mol to substrate-binding energy (Pyle et al., 1992; Strobel & Cech, 1993), stabilizing tertiary contacts might also occur between the two helix−loop−helix domains of the hairpin. However, interactions between domains were not evident in cross-linking or chemical modification experiments (Vitorino Dos Santos et al., 1993; Butcher & Burke, 1994a,b).

The rate constant for S2−P2 binding, k_{-4}, was somewhat slower than typical rate constants for RNA helix formation (Pörschke & Eigen, 1971; Craig et al., 1971; Pörschke et al., 1973; Ravetch et al., 1974) but fell within the range previously measured for product binding to *Tetrahymena*, hammerhead, and RNase P ribozymes (Herschlag & Cech, 1990; Fedor & Uhlenbeck, 1992; Hertel et al., 1994; Beebe & Fierke, 1994). S2−P2 dissociation rate constants were significantly slower than expected for a short RNA duplex with the same length and sequence, consistent with the enhanced binding energy observed for all 3′-cleavage products. In this regard, the R1/S2 and R5/S6 hairpins resemble the *Tetrahymena* ribozyme for which enhanced stability of the ribozyme−product complex is reflected in slow product dissociation. Although aggregation of S2 and S6 RNAs precluded experiments at the high substrate concentrations needed for direct measurement of multiple-turnover cleavage rates, the rate constant for dissociation of S2−P2 was more than 3 orders of magnitude slower than the cleavage rate constant. Therefore, slow S2−P2 dissociation would limit multiple-turnover cleavage rates at saturating concentrations. Slow product release has also been found to limit multiple-turnover reactions of *Tetrahymena* (Herschlag & Cech, 1990), RNase P (Smith & Pace, 1993; Beebe & Fierke, 1994), and some hammerhead ribozymes (Fedor & Uhlenbeck, 1992; Hertel et al., 1994).

Analysis of substrate dissociation kinetics was complicated by the contradictory results of experiments that monitored partitioning between cleavage and dissociation of ribozyme−substrate complexes formed either through substrate binding or through product ligation reactions. While complexes that formed in binding reactions appeared to dissociate at rates comparable to cleavage rates, complexes formed in ligation reactions dissociated too slowly to detect under standard conditions. The conclusion from ligation−chase experiments, that substrate dissociation is much slower than cleavage, is likely to be correct because complexes formed through ligation must be functional whereas nonfunctional, lower affinity complexes could form at the high concentrations required for rapid binding reactions. Initial experiments designed to measure the rate of R1·S2−P2 dissociation gave some indication of an alternate, low-affinity S2−P2 binding mode. When the R1·S2−P2 complex was formed with 1 μM R1, a concentration $\sim 1 \times 10^5$ higher than the concentration required for complete binding, dissociation occurred in two distinct phases with 80% of the complex dissociated after 2 h while the remainder failed to dissociate by the end of the time course (data not shown). Similar low-affinity substrate binding could account for the rapid substrate dissociation detected in partitioning experiments that were initiated by substrate binding reactions at high concentrations. Another reason to conclude that ligation−chase experiments gave a more accurate measure of substrate dissociation is that slow substrate dissociation rates are consistent with the similarity among all substrates in cleavage kinetics. K_M^S will approach a constant value of k_2/k_1 and will not equal k_{-1}/k_1, or K_d^S, when substrate dissociation rate constants are small compared to cleavage rate constants (eq 1). Thus, the virtual identity of K_M^S values among substrates that were expected to bind ribozyme with very different affinities indicated that K_M^S was not equal to K_d^S and that k_{-1} must be small relative to k_2 for all substrates.

An equilibrium dissociation constant of 0.8 nM can be calculated for the R1/S4 hairpin complex from the ratio of the dissociation rate constant, measured through ligation−chase experiments at pH 5.5, and the binding rate constant of 1.3×10^7 calculated from the ratio of k_2 and K_M^S values (Table 1). Although substrate dissociation rates could be different at pH 5.5 and 7.5, any effect of reduced pH on dissociation is expected to be small since the ionization state of ribonucleosides is the same at pH 5.5 and 7.5 (Saenger, 1984). The K_d^{S4} value corresponds to a binding energy for R1·S4 of −12.4 kcal/mol. Binding energies for S4−P1 and S4−P2 were too weak to be measured directly but can be estimated by assuming that all hairpin E·P1 and E·P2 complexes will deviate by the same amount from the binding energy calculated for corresponding helices. Based on equilibrium dissociation constants that were measured for S5−P1, S1−P2, S2−P2, and S3−P2 (Table 2), hairpin product binding energies can be described by $\Delta G_{25\ ^\circ C}^{E\cdot P1} = \Delta G_{25\ ^\circ C}^{P1\ helix} + 0.8$ kcal/mol and $\Delta G_{25\ ^\circ C}^{E\cdot P2} = \Delta G_{25\ ^\circ C}^{P2\ helix} - 2.5$ kcal/mol. This calculation gives binding energies of −5.4 and −7.4 kcal/mol for S4−P1 and S4−P2 complexes, respectively. Because binding of one cleavage product did not detectably affect binding of the other, the binding energy of the R1·S4−P1·S4−P2 ternary complex can be estimated from the sum of the binding energies of each product, which totals −12.8 kcal/mol. Thus, E·S, with a binding energy of −12.4 kcal/mol, appears to be nearly energetically equivalent to E·P1·P2, consistent with an equilibrium between cleavage and ligation near 1. While a major conformational change accompanying the chemical step has not been excluded, the similarity in binding energy between E·S and E·P1·P2 suggests that the two have similar structures.

Implications of the Kinetic Mechanism for Antisense Applications and Structure−Function Studies. Elucidation of the hairpin kinetic mechanism points to the importance of substrate and product binding affinities in the optimization of hairpin ribozymes designed to cleave heterologous targets efficiently and specifically. When the ribozyme binds substrate with high affinity, K_M^S approaches a constant value,

~30 nM under the reaction conditions used here, which is the ratio of cleavage and substrate binding rate constants and not the ratio of substrate dissociation and binding rate constants, K_d^S. Consequently, ribozymes designed to bind targets with high affinity will not discriminate against related target sequences that, in spite of binding with lower affinity, will still dissociate more slowly than they cleave [for discussion, see Herschlag (1991) and Fedor and Uhlenbeck (1992)]. High-affinity binding of cleavage products will not only result in slow multiple-turnover cleavage rates, due to slow product dissociation, but also could reduce apparent cleavage rates during the first turnover. If both products remain bound to the ribozyme long enough to undergo ligation or accumulate at concentrations high enough to promote ternary complex formation, then maximum cleavage rates, even during the first turnover, will reflect a balance between cleavage and ligation and the final extent of cleavage will reflect the equilibrium between the two. Thus, to maximize single- and multiple-turnover cleavage efficiency and reduce nonspecific cleavage, it appears that the intermolecular helices between ribozymes and antisense targets should be designed to have the minimum length needed to ensure that the target sequence is unique.

The two most important features of the kinetic mechanism with regard to structure–function studies are the nonequivalence of K_M^S and K_d^S and the preference for ligation over cleavage at saturating concentrations because these features affect the interpretation of steady-state kinetics parameters. In particular, because $K_M^S = (k_{-1} + k_2)/k_1$, structural perturbations that affect substrate binding affinity will have no effect on K_M^S values unless the change in affinity is so large that k_{-1} becomes faster than k_2. For the S4 substrate sequence with a dissociation rate constant $k_{-1} \leq 0.01$ min^{-1}, for example, a 30-fold change in K_d^S would be expected to increase K_M^S only 2-fold because k_{-1} and k_2 values would become approximately equal. For substrates that bind with higher affinity than S4 and have slower dissociation rate constants, the magnitude of change in K_d^S required to observe a change in K_M^S would increase proportionately. Furthermore, when k_{-1} is small compared to k_2, so that $K_M^S \approx k_2/k_1$, perturbations that reduce k_2 would reduce K_M^S proportionately even if substrate binding affinity was unchanged. Finally, as discussed above, observed cleavage rates will reflect the balance between cleavage and ligation, and not cleavage alone, under conditions that allow accumulation of a ternary complex containing the ribozyme and both products. When cleavage products bind with high affinity and dissociate slowly, ligation within a stable ternary complex will reduce apparent cleavage rates even under single-turnover conditions.

The application of pre-steady-state kinetics to Group I intron-derived and hammerhead ribozyme reactions has led to a new level of understanding of these RNA-catalyzed reactions [reviewed in Long and Uhlenbeck (1993), Cech (1993), and Pyle (1993)]. Recent investigations of the kinetic mechanisms of Group II intron- and RNase P-derived ribozymes (Franzen et al., 1993; Pyle & Green, 1994; Smith & Pace, 1993; Beebe & Fierke, 1994) and now the hairpin ribozyme promise to provide equally useful tools for understanding these reactions as well.

ACKNOWLEDGMENT

We thank Christine Donahue for helpful discussions and Jamie Williamson and Pat Zarrinkar for critical reading of the manuscript.

REFERENCES

Anderson, P., Monforte, J., Tritz, R., Nesbitt, S., Hearst, J., & Hampel. A. (1994) *Nucleic Acids Res. 22*, 1096–1100.
Beebe, J. A., & Fierke, C. A. (1994) *Biochemistry 33*, 10294–10304.
Berzal-Herranz, A., Joseph, S., & Burke, J. M. (1992) *Genes Dev. 6*, 129–134.
Berzal-Herranz, A., Joseph, S., Chowrira, B. M., Butcher, S. E., & Burke, J. M. (1993) *EMBO J. 12*, 2567–2573.
Bevilacqua, P. C., & Turner, D. H. (1991) *Biochemistry 30*, 10632–10640.
Butcher, S. E., & Burke, J. M. (1994a) *Biochemistry 33*, 992–999.
Butcher, S. E., & Burke, J. M. (1994b) *J. Mol. Biol. 244*, 52–63.
Buzayan, J. M., Gerlach, W. L., Bruening, G., Keese, P., & Gould, A. R. (1986a) *Virology 151*, 186–199.
Buzayan, J. M., Gerlach, W. L., & Bruening, G. (1986b) *Nature 323*, 349–353.
Buzayan, J. M., Feldstein, P. A., Bruening, G., & Eckstein, F. (1988) *Biochem. Biophys. Res. Commun. 156*, 340–347.
Cech, T. R. (1993) in *The RNA World* (Gesteland, R. F., & Atkins, J. F., Eds.) pp 239–269, Cold Spring Harbor Laboratory Press, Cold Spring Harbor, NY.
Chowrira, B. H., & Burke, J. M. (1991) *Biochemistry 30*, 8518–8522.
Chowrira, B. H., Berzal-Herranz, A., Keller, C. F., & Burke, J. M. (1993) *J. Biol. Chem. 268*, 19458–19462.
Craig, M. E., Crothers, D. M., & Doty, P. (1971) *J. Mol. Biol. 62*, 383–401.
Dahm, S. C., & Uhlenbeck, O. C. (1991) *Biochemistry 30*, 9464–9469.
Dahm, S. C., Derrick, W. B., & Uhlenbeck, O. C. (1993) *Biochemistry 32*, 13040–13045.
Eadie, G. S. (1942) *J. Mol. Biol. 146*, 85–93.
England, T. E., & Uhlenbeck, O. C. (1988) *Biochemistry 17*, 2069–2076.
Fedor, M. J., & Uhlenbeck, O. C. (1990) *Proc. Natl. Acad. Sci. U.S.A. 87*, 1668–1672.
Fedor, M. J., & Uhlenbeck, O. C. (1992) *Biochemistry 31*, 12042–12054.
Feldstein, P. A., & Bruening, G. (1993) *Nucleic Acids Res. 21*, 1991–1998.
Feldstein, P. A., Buzayan, J. M., & Bruening, G. (1989) *Gene 82*, 53–61.
Feldstein, P. A., Buzayan, J. M., van Tol, H., deBear, J., Gough, G. R., Gilham, P. T., & Bruening, G. (1990) *Proc. Natl. Acad. Sci. U.S.A. 87*, 2623–2627.
Forster, A. C., Jeffries, A. C., Sheldon, C. C., & Symons, R. H. (1987) *Cold Spring Harbor Symp. Quant. Biol. 52*, 249–259.
Franzen, J. S., Zhang, M., & Peebles, C. L. (1993) *Nucleic Acids Res. 21*, 627–634.
Gerlt, J. A., Westheimer, F. H., & Surtevant, J. M. (1975) *J. Biol. Chem. 250*, 5059–5067.
Grasby, J. A., Mersmann, K., Singh, M., & Gait, M. J. (1995) *Biochemistry 34*, 4068–4076.
Groebe, D. R., & Uhlenbeck, O. C. (1988) *Nucleic Acids Res. 16*, 11725–11735.
Hampel. A., & Tritz, R. (1989) *Biochemistry 28*, 4929–4933.
Hampel. A., Tritz, R., Hicks, M., & Cruz, P. (1990) *Nucleic Acids Res. 18*, 299–304.
Haseloff, J., & Gerlach, W. L. (1988) *Nature 334*, 585–591.
Haseloff, J., & Gerlach, W. L. (1989) *Gene 82*, 43–52.
Herschlag, D. (1991) *Proc. Natl. Acad. Sci. U.S.A. 88*, 6921–6925.
Herschlag, D., & Cech, T. R. (1990) *Biochemistry 29*, 10159–10171.
Hertel, K. J., & Uhlenbeck, O. C. (1995) *Biochemistry 34*, 1744–1749.

Hertel, K. J., Herschlag, D., & Uhlenbeck, O. C. (1994) *Biochemistry 33*, 3374−3385.
Hofstee, B. H. J. (1952) *J. Biol. Chem. 199*, 357−364.
Hutchins, C. J., Rathjen, P. D., Forster, A. C., & Symons, R. H. (1986) *Nucleic Acids Res. 14*, 3627−3640.
Jeffries, A. C., & Symons, R. H. (1989) *Nucleic Acids Res. 17*, 1371−1377.
Joseph, S., Berzal-Herranz, A., Chowrira, B. M., & Burke, J. M. (1993) *Genes Dev. 7*, 130−138.
Kochino, Y., Wantanabe, S., Harada, F., & Nishimura, S. (1980) *Biochemistry 19*, 2085−2089.
Koizumi, M., & Ohtsuka, E. (1991) *Biochemistry 30*, 5145−5150.
Koizumi, M., Iwai, S., & Ohtsuka, E. (1988a) *FEBS Lett. 228*, 228−230.
Koizumi, M., Iwai, S., & Ohtsuka, E. (1988b) *FEBS Lett. 229*, 285−288.
Komatsu, Y., Koizumi, M., Sekiguchi, A., & Ohtsuka, E. (1993) *Nucleic Acids Res. 21*, 185−190.
Komatsu, Y., Koizumi, M., Nakamura, H., & Ohtsuka, E. (1994) *J. Am. Chem. Soc. 116*, 3692−3696.
Long, D. M., & Uhlenbeck, O. C. (1993) *FASEB J. 7*, 25−30.
Milligan, J. F., Groebe, D. R., Witherell, G. W., & Uhlenbeck, O. C. (1987) *Nucleic Acids Res. 15*, 8783−8798.
Naylor, R., & Gilham, P. T. (1966) *Biochemistry 5*, 2722−2726.
Perrota, A. T., & Been, M. D. (1992) *Biochemistry 31*, 16−21
Pörschke, D., & Eigen, M. (1971) *J. Mol. Biol. 62*, 361−381.
Pörschke, D., Uhlenbeck, O. C., & Martin, M. F. (1973) *Biopolymers 12*, 1313−1335.
Prody, G. A., Bakos, J. T., Buzayan, J. M., Schneider, I. R., & Bruening, G. (1986) *Science 231*, 1577−1580.
Pyle A. M. (1993) *Science 261*, 709−714.
Pyle, A. M., & Cech, T. R. (1991) *Nature 350*, 628−630.
Pyle, A. M., Murphy, F. L., & Cech, T. R. (1992) *Nature 258*, 123−128.
Pyle, A. M., & Green, J. B.(1994) *Biochemistry 33*, 2716−2725.
Pyle, A. M., McSwiggen, J. A., & Cech, T. R. (1990) *Proc. Natl. Acad. Sci. U.S.A. 87*, 8187−8191.
Pyle, A. M., & Cech, T. R. (1992) *Nature 358*, 123−128.
Ravetch, J., Gralla, J., & Crothers, D. M. (1974) *Nucleic Acids Res. 1*, 109−127.
Rose, I. A., O'Connell, E. L., Litwin, S., & Bar Tana, J. (1974) *J. Biol. Chem. 249*, 5163−5168.
Rubino, L., Tousignant, M. E., Steger, G., & Kaper, J. M. (1990) *J. Gen. Virol. 71*, 1897−1903.
Saenger, W. (1984) *Principles of Nucleic Acid Structure*, Springer-Verlag, New York.
Sampson, J. R., Sullivan, F. X., Behlen, L. S., DiRenzo, A. B., & Uhlenbeck, O. C. (1987) *Cold Spring Harbor Symp. Quant. Biol. 52*, 267−275.
SantaLucia, J., Jr., Kierzek, R., & Turner, D. H. (1990) *Biochemistry 29*, 8813−8819.
Sekiguchi, A., Komatsu, Y., Koizumi, M., & Ohtsuka, E. (1991) *Nucleic Acids Res. 19*, 6833−6838.
Smith, D., & Pace, N. R. (1993) *Biochemistry 32*, 5273−5281.
Strobel, S. A., & Cech, T. R. (1993) *Biochemistry 32*, 13596−13604.
Sugimoto, N., Kierzek, M. R., & Turner, D. H. (1988) *Biochemistry 27*, 6384−6392.
Sugimoto, N., Sasaki, M., Kierzek, R., & Turner, D. H. (1989) *Chem. Lett.* 2223−2226.
Sullivan, F. X., & Cech, T. R. (1985) *Cell 42*, 639−648.
Symons, R. H. (1992) *Annu. Rev. Biochem. 61*, 641−671.
Turner, D. H., Sugimoto, N., & Freier, S. M. (1988) *Annu. Rev. Biophys. Biophys. Chem. 17*, 167−192.
Uhlenbeck, O. C. (1987) *Nature 328*, 596−600.
van Tol, H., Buzayan, J. M., & Bruening, G. (1991) *Virology 180*, 23−30.
Vitorino Dos Santos, D., Vianna, A.-L., Fourrey, J.-L., & Favre, A. (1993) *Nucleic Acids Res. 21*, 201−207.
Wu, M., McDowell, J. A., & Turner, D. H. (1995) *Biochemistry 34*, 3204−3211.
Zaug, A. J., Davila-Aponte, J. A., & Cech, T. R. (1994) *Biochemistry 33*, 14935−14947.

BI951549R